CHAPTER 5

Electromagnetic Potentials and Topics for Circuits and Systems

In Chapters 2, 3, and 4, we introduced progressively Maxwell's equations and studied uniform plane waves and associated topics. Two quantities of fundamental importance, resulting from Maxwell's equations in differential form, are the electromagnetic potentials: the electric scalar potential and the magnetic vector potential. We introduce these quantities in this chapter and also consider several topics of relevance to circuits and systems.

We begin the discussion of topics for circuits and systems with two important differential equations involving the electric potential and discuss several applications based on the solution of these equations, including the analysis of a *p-n* junction semiconductor and arrangements involving two parallel conductors. We then introduce an important relationship between the (lumped) circuit parameters, capacitance, conductance, and inductance for infinitely long, parallel perfect conductor arrangements, and consider their determination.

Next we turn our attention to electric- and magnetic-field systems, that is, systems in which either the electric field or the magnetic field is predominant, leading from *quasistatic* extensions of the static fields existing in the structures when the frequency of the source driving the structure is zero. The concepts of electric- and magnetic-field systems are important in the study of electromechanics. We shall also consider magnetic circuits, an important class of magnetic field systems, and the topic of electromechanical energy conversion.

5.1 GRADIENT, LAPLACIAN, AND THE POTENTIAL FUNCTIONS

Magnetic vector potential

In Example 3.9, we showed that for any vector $\mathbf{A}$, $\nabla \cdot \nabla \times \mathbf{A} = 0$. It then follows from Gauss' law for the magnetic field in differential form, $\nabla \cdot \mathbf{B} = 0$, that the magnetic flux density vector $\mathbf{B}$ can be expressed as the curl of another vector **A**; that is,

$$\boxed{\mathbf{B} = \nabla \times \mathbf{A}} \tag{5.1}$$

The vector **A** in (5.1) is known as the *magnetic vector potential*.

Substituting (5.1) into Faraday's law in differential form, $\nabla \times \mathbf{E} = -\partial \mathbf{B}/\partial t$, and rearranging, we then obtain *Gradient*

$$\nabla \times \mathbf{E} + \frac{\partial}{\partial t}(\nabla \times \mathbf{A}) = \mathbf{0}$$

or

$$\nabla \times \left(\mathbf{E} + \frac{\partial \mathbf{A}}{\partial t}\right) = \mathbf{0} \tag{5.2}$$

If the curl of a vector is equal to the null vector, that vector can be expressed as the *gradient* of a scalar, since the curl of the gradient of a scalar function is identically equal to the null vector. The gradient of a scalar, say, Φ, denoted $\nabla\Phi$ (del Φ) is defined in such a manner that the increment $d\Phi$ in Φ from a point P to a neighboring point Q is given by

$$d\Phi = \nabla\Phi \cdot d\mathbf{l} \tag{5.3}$$

where $d\mathbf{l}$ is the differential length vector from P to Q. Applying Stokes' theorem to the vector $\nabla \times \nabla\Phi$ and a surface S bounded by closed path C, we then have

$$\begin{aligned} \int_S (\nabla \times \nabla\Phi) \cdot d\mathbf{S} &= \oint_C \nabla\Phi \cdot d\mathbf{l} \\ &= \oint_C d\Phi \\ &= 0 \end{aligned} \tag{5.4}$$

for any single-valued function Φ. Since (5.4) holds for an arbitrary S, it follows that

$$\boxed{\nabla \times \nabla\Phi = \mathbf{0}} \tag{5.5}$$

To obtain the expression for the gradient in the Cartesian coordinate system, we write

$$\begin{aligned} d\Phi &= \frac{\partial\Phi}{\partial x}dx + \frac{\partial\Phi}{\partial y}dy + \frac{\partial\Phi}{\partial z}dz \\ &= \left(\frac{\partial\Phi}{\partial x}\mathbf{a}_x + \frac{\partial\Phi}{\partial y}\mathbf{a}_y + \frac{\partial\Phi}{\partial z}\mathbf{a}_z\right) \cdot (dx\,\mathbf{a}_x + dy\,\mathbf{a}_y + dz\,\mathbf{a}_z) \end{aligned} \tag{5.6}$$

Then comparing with (5.3), we observe that

$$\boxed{\nabla\Phi = \frac{\partial\Phi}{\partial x}\mathbf{a}_x + \frac{\partial\Phi}{\partial y}\mathbf{a}_y + \frac{\partial\Phi}{\partial z}\mathbf{a}_z} \tag{5.7}$$

Note that the right side of (5.7) is simply the vector obtained by applying the del operator to the scalar function Φ. It is for this reason that the gradient of Φ is written as $\nabla\Phi$. Expressions for the gradient in cylindrical and spherical coordinate systems are derived in Appendix B. These are as follows:

CYLINDRICAL

$$\nabla\Phi = \frac{\partial\Phi}{\partial r}\mathbf{a}_r + \frac{1}{r}\frac{\partial\Phi}{\partial\phi}\mathbf{a}_\phi + \frac{\partial\Phi}{\partial z}\mathbf{a}_z \tag{5.8a}$$

SPHERICAL

$$\nabla\Phi = \frac{\partial\Phi}{\partial r}\mathbf{a}_r + \frac{1}{r}\frac{\partial\Phi}{\partial\theta}\mathbf{a}_\theta + \frac{1}{r\sin\theta}\frac{\partial\Phi}{\partial\phi}\mathbf{a}_\phi \tag{5.8b}$$

Physical interpretation of gradient

To discuss the physical interpretation of the gradient, let us consider a surface on which Φ is equal to a constant, say, Φ_0, and a point P on that surface, as shown in Fig. 5.1(a). If we now consider another point Q_1 on the same surface and an infinitesimal distance away from P, $d\Phi$ between these two points is zero since Φ is constant on the surface. Thus, for the vector $d\mathbf{l}_1$ drawn from P to Q_1, $[\nabla\Phi]_P \cdot d\mathbf{l}_1 = 0$ and hence $[\nabla\Phi]_P$ is perpendicular to $d\mathbf{l}_1$. Since this is true for

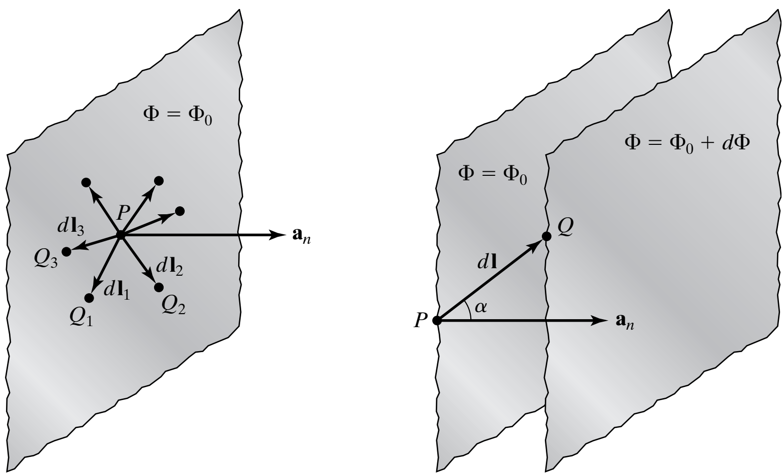

(a) (b)

FIGURE 5.1

For discussing the physical interpretation of the gradient of a scalar function.

all points $Q_1, Q_2, Q_3, \ldots$ on the constant Φ surface, it follows that $[\nabla\Phi]_P$ must be normal to all possible infinitesimal length vectors $d\mathbf{l}_1, d\mathbf{l}_2, d\mathbf{l}_3, \ldots$ drawn at P and hence is normal to the surface. Denoting $\mathbf{a}_n$ to be the unit normal vector to the surface at P, we then have

$$[\nabla\Phi]_P = |\nabla\Phi|_P \mathbf{a}_n \tag{5.9}$$

Let us now consider two surfaces on which Φ is constant, having values Φ_0 and $\Phi_0 + d\Phi$, as shown in Fig. 5.1(b). Let P and Q be points on the $\Phi = \Phi_0$ and $\Phi = \Phi_0 + d\Phi$ surfaces, respectively, and $d\mathbf{l}$ be the vector drawn from P to Q. Then from (5.3) and (5.9),

$$\begin{aligned} d\Phi &= [\nabla\Phi]_P \cdot d\mathbf{l} \\ &= |\nabla\Phi|_P \mathbf{a}_n \cdot d\mathbf{l} \\ &= |\nabla\Phi|_P \, dl \cos\alpha \end{aligned}$$

where α is the angle between $\mathbf{a}_n$ at P and $d\mathbf{l}$. Thus,

$$|\nabla\Phi|_P = \frac{d\Phi}{dl\cos\alpha} \tag{5.10}$$

Since $dl \cos\alpha$ is the distance between the two surfaces along $\mathbf{a}_n$ and hence is the shortest distance between them, it follows that $|\nabla\Phi|_P$ is the maximum rate of increase of Φ at the point P. Thus, the gradient of a scalar function Φ at a point is a vector having magnitude equal to the maximum rate of increase of Φ at that point and is directed along the direction of the maximum rate of increase, which is normal to the constant Φ surface passing through that point; that is,

$$\boxed{\nabla\Phi = \frac{d\Phi}{dn}\mathbf{a}_n} \tag{5.11}$$

where dn is a differential length along $\mathbf{a}_n$. The concept of the gradient of a scalar function we just discussed is often utilized to find a unit vector normal to a given surface. We shall illustrate this by means of an example.

Example 5.1 Finding unit vector normal to a surface by using the gradient concept

Let us find the unit vector normal to the surface $y = x^2$ at the point $(2, 4, 1)$ by using the concept of the gradient of a scalar.

Writing the equation for the surface as

$$x^2 - y = 0$$

we note that the scalar function that is constant on the surface is given by

$$\Phi(x, y, z) = x^2 - y$$

The gradient of the scalar function is then given by

$$\begin{aligned}\nabla\Phi &= \nabla(x^2 - y)\\ &= \frac{\partial(x^2 - y)}{\partial x}\mathbf{a}_x + \frac{\partial(x^2 - y)}{\partial y}\mathbf{a}_y + \frac{\partial(x^2 - y)}{\partial z}\mathbf{a}_z\\ &= 2x\mathbf{a}_x - \mathbf{a}_y\end{aligned}$$

The value of the gradient at the point (2, 4, 1) is $[2(2)\mathbf{a}_x - \mathbf{a}_y] = (4\mathbf{a}_x - \mathbf{a}_y)$. Thus, the required unit vector is

$$\mathbf{a}_n = \pm\frac{4\mathbf{a}_x - \mathbf{a}_y}{|4\mathbf{a}_x - \mathbf{a}_y|} = \pm\left(\frac{4}{\sqrt{17}}\mathbf{a}_x - \frac{1}{\sqrt{17}}\mathbf{a}_y\right)$$

Electric scalar potential

Returning now to (5.2), we write

$$\mathbf{E} + \frac{\partial\mathbf{A}}{\partial t} = -\nabla\Phi \tag{5.12}$$

where we have chosen the scalar to be $-\Phi$, the reason for the minus sign to be explained in Section 5.2. Rearranging (5.12), we obtain

$$\boxed{\mathbf{E} = -\nabla\Phi - \frac{\partial\mathbf{A}}{\partial t}} \tag{5.13}$$

The quantity Φ in (5.13) is known as the electric scalar potential.

Electromagnetic potentials

The electric scalar potential Φ and the magnetic vector potential $\mathbf{A}$ are known as the electromagnetic potentials. As we shall show later in this section, the electric scalar potential is related to the source charge density ρ, whereas the magnetic vector potential is related to the source current density $\mathbf{J}$. For the time-varying case, the two are not independent, since the charge and current densities are related through the continuity equation. For a given $\mathbf{J}$, it is sufficient to determine $\mathbf{A}$, since $\mathbf{B}$ can be found from (5.1) and then $\mathbf{E}$ can be found by using Ampère's circuital law $\nabla \times \mathbf{H} = \mathbf{J} + \partial\mathbf{D}/\partial t$. For static fields, that is, for $\partial/\partial t = 0$, the two potentials are independent. Equation (5.1) remains unaltered, whereas (5.13) reduces to $\mathbf{E} = -\nabla\Phi$. We shall consider the static field case in Section 5.2.

To proceed further, we recall that Maxwell's equations in differential form are given by

$$\nabla \times \mathbf{E} = -\frac{\partial\mathbf{B}}{\partial t} \tag{5.14a}$$

$$\nabla \times \mathbf{H} = \mathbf{J} + \frac{\partial\mathbf{D}}{\partial t} \tag{5.14b}$$

$$\nabla\cdot\mathbf{D} = \rho \tag{5.14c}$$

$$\nabla\cdot\mathbf{B} = 0 \tag{5.14d}$$

From (5.14d), we expressed **B** in the manner

$$\mathbf{B} = \nabla \times \mathbf{A} \tag{5.15}$$

and then from (5.14a), we obtained

$$\mathbf{E} = -\nabla\Phi - \frac{\partial \mathbf{A}}{\partial t} \tag{5.16}$$

We now substitute (5.16) and (5.15) into (5.14c) and (5.14b), respectively, to obtain

$$\nabla \cdot \left(-\nabla\Phi - \frac{\partial \mathbf{A}}{\partial t}\right) = \frac{\rho}{\varepsilon} \tag{5.17a}$$

$$\nabla \times \nabla \times \mathbf{A} - \mu\varepsilon\frac{\partial}{\partial t}\left(-\nabla\Phi - \frac{\partial \mathbf{A}}{\partial t}\right) = \mu\mathbf{J} \tag{5.17b}$$

Laplacian of a scalar

We now define the Laplacian of a scalar quantity Φ, denoted $\nabla^2\Phi$ (del squared Φ) as

$$\boxed{\nabla^2\Phi = \nabla \cdot \nabla\Phi} \tag{5.18}$$

In Cartesian coordinates,

$$\nabla\Phi = \frac{\partial \Phi}{\partial x}\mathbf{a}_x + \frac{\partial \Phi}{\partial y}\mathbf{a}_y + \frac{\partial \Phi}{\partial z}\mathbf{a}_z$$

$$\nabla \cdot \mathbf{A} = \frac{\partial A_x}{\partial x} + \frac{\partial A_y}{\partial y} + \frac{\partial A_z}{\partial z}$$

so that

$$\nabla^2\Phi = \frac{\partial}{\partial x}\left(\frac{\partial \Phi}{\partial x}\right) + \frac{\partial}{\partial y}\left(\frac{\partial \Phi}{\partial y}\right) + \frac{\partial}{\partial z}\left(\frac{\partial \Phi}{\partial z}\right)$$

or

$$\boxed{\nabla^2\Phi = \frac{\partial^2 \Phi}{\partial x^2} + \frac{\partial^2 \Phi}{\partial y^2} + \frac{\partial^2 \Phi}{\partial z^2}} \tag{5.19}$$

Note that the Laplacian of a scalar is a scalar quantity. Expressions for the Laplacian of a scalar in cylindrical and spherical coordinates are derived in Appendix B. These are as follows:

CYLINDRICAL

$$\nabla^2\Phi = \frac{1}{r}\frac{\partial}{\partial r}\left(r\frac{\partial \Phi}{\partial r}\right) + \frac{1}{r^2}\frac{\partial^2 \Phi}{\partial \phi^2} + \frac{\partial^2 \Phi}{\partial z^2} \tag{5.20a}$$

Spherical

$$\nabla^2\Phi = \frac{1}{r^2}\frac{\partial}{\partial r}\left(r^2\frac{\partial\Phi}{\partial r}\right) + \frac{1}{r^2\sin\theta}\frac{\partial}{\partial\theta}\left(\sin\theta\frac{\partial\Phi}{\partial\theta}\right) + \frac{1}{r^2\sin^2\theta}\frac{\partial^2\Phi}{\partial\phi^2} \tag{5.20b}$$

Before proceeding further, it is interesting to note that the four vector differential operations that we have learned thus far in this chapter are such that

The *curl* of a *vector* is a *vector*.
The *divergence* of a *vector* is a *scalar*.
The *gradient* of a *scalar* is a *vector*.
The *Laplacian* of a *scalar* is a *scalar*.

Thus, all four combinations of vector and scalar are involved in the four operations.

Laplacian of a vector

Next, we define the Laplacian of a vector, denoted $\nabla^2\mathbf{A}$ as

$$\boxed{\nabla^2\mathbf{A} = \boldsymbol{\nabla}(\boldsymbol{\nabla}\cdot\mathbf{A}) - \boldsymbol{\nabla}\times\boldsymbol{\nabla}\times\mathbf{A}} \tag{5.21}$$

Expanding the right side of (5.21) in Cartesian coordinates and simplifying, we obtain in the Cartesian coordinate system,

$$\boxed{\nabla^2\mathbf{A} = (\nabla^2 A_x)\mathbf{a}_x + (\nabla^2 A_y)\mathbf{a}_y + (\nabla^2 A_z)\mathbf{a}_z} \tag{5.22}$$

Thus, in the Cartesian coordinate system, the Laplacian of a vector is a vector whose components are the Laplacians of the corresponding components of **A**. It should, however, be cautioned that this simple observation does not hold in the cylindrical and spherical coordinate systems. (See, e.g., Problem P5.6.)

Using (5.18) and (5.21), we now write (5.17a) and (5.17b) as

$$\nabla^2\Phi + \frac{\partial}{\partial t}(\boldsymbol{\nabla}\cdot\mathbf{A}) = -\frac{\rho}{\varepsilon} \tag{5.23a}$$

$$\nabla^2\mathbf{A} - \boldsymbol{\nabla}\left(\boldsymbol{\nabla}\cdot\mathbf{A} + \mu\varepsilon\frac{\partial\Phi}{\partial t}\right) - \mu\varepsilon\frac{\partial^2\mathbf{A}}{\partial t^2} = -\mu\mathbf{J} \tag{5.23b}$$

Potential function equations

Equations (5.23a) and (5.23b) are a pair of coupled differential equations for Φ and **A**. To uncouple the equations, we make use of a theorem known as Helmholtz's theorem, which states that a vector field is completely specified by its curl and divergence. Therefore, since the curl of **A** is given by (5.15), we are at liberty to specify the divergence of **A**. We do this by setting

$$\boxed{\boldsymbol{\nabla}\cdot\mathbf{A} = -\mu\varepsilon\frac{\partial\Phi}{\partial t}} \tag{5.24}$$

which is known as the Lorenz condition[1]. This uncouples (5.23a) and (5.23b) to give us

$$\boxed{\begin{aligned} \nabla^2\Phi - \mu\varepsilon\frac{\partial^2\Phi}{\partial t^2} &= -\frac{\rho}{\varepsilon} \\ \nabla^2\mathbf{A} - \mu\varepsilon\frac{\partial^2\mathbf{A}}{\partial t^2} &= -\mu\mathbf{J} \end{aligned}} \quad \begin{aligned} (5.25) \\ (5.26) \end{aligned}$$

These are the differential equations relating the electromagnetic potentials Φ and $\mathbf{A}$ to the source charge and current densities ρ and $\mathbf{J}$, respectively.

Before proceeding further, we shall show that the continuity equation is implied by the Lorenz condition. To do this, we take the Laplacian of both sides of (5.24). We then have

$$\nabla^2(\boldsymbol{\nabla}\cdot\mathbf{A}) = -\mu\varepsilon\nabla^2\frac{\partial\Phi}{\partial t}$$

or

$$\boldsymbol{\nabla}\cdot\nabla^2\mathbf{A} = -\mu\varepsilon\frac{\partial}{\partial t}\nabla^2\Phi \tag{5.27}$$

Substituting for $\nabla^2\mathbf{A}$ and $\nabla^2\Phi$ in (5.27) from (5.26) and (5.25), respectively, we get

$$\boldsymbol{\nabla}\cdot\left(\mu\varepsilon\frac{\partial^2\mathbf{A}}{\partial t^2} - \mu\mathbf{J}\right) = -\mu\varepsilon\frac{\partial}{\partial t}\left(\mu\varepsilon\frac{\partial^2\Phi}{\partial t^2} - \frac{\rho}{\varepsilon}\right)$$

or

$$\mu\varepsilon\frac{\partial^2}{\partial t^2}\left(\boldsymbol{\nabla}\cdot\mathbf{A} + \mu\varepsilon\frac{\partial\Phi}{\partial t}\right) = \mu\left(\boldsymbol{\nabla}\cdot\mathbf{J} + \frac{\partial\rho}{\partial t}\right) \tag{5.28}$$

Thus, by assuming the Lorenz condition (5.24), we imply $\boldsymbol{\nabla}\cdot\mathbf{J} + \partial\rho/\partial t = 0$, which is the continuity equation.

As pointed out earlier in this section, it is sufficient to determine $\mathbf{A}$ for the time-varying case for a given $\mathbf{J}$. Hence, we shall be concerned only with (5.26), which we shall refer to in Section 10.1 in connection with obtaining the electromagnetic field due to an elemental antenna.

K5.1. Magnetic vector potential; Gradient of a scalar; Physical interpretation of gradient; Electric scalar potential; Laplacian of a scalar; Potential function equations.

---

[1]Note "Lorenz condition" and not "Lorentz condition." In editions 2, 3, and 4 of this book, as well as extensively in books by other authors, this condition has been mistakenly attributed to Lorentz instead of Lorenz. See the note "Lorentz or Lorenz," by J. Van Bladel in *IEEE Antennas and Propagation Magazine*, Vol. 33, No. 2, April 1991, p. 69.

D5.1. Find the outward pointing unit vectors normal to the closed surface $2x^2 + 2y^2 + z^2 = 8$ at the following points: **(a)** $(\sqrt{2}, \sqrt{2}, 0)$; **(b)** $(1, 1, 2)$; and **(c)** $(1, \sqrt{2}, \sqrt{2})$.

Ans. **(a)** $\dfrac{\mathbf{a}_x + \mathbf{a}_y}{\sqrt{2}}$; **(b)** $\dfrac{\mathbf{a}_x + \mathbf{a}_y + \mathbf{a}_z}{\sqrt{3}}$ **(c)** $\dfrac{\sqrt{2}\mathbf{a}_x + 2\mathbf{a}_y + \mathbf{a}_z}{\sqrt{7}}$

D5.2. Two scalar functions are given by

$$\Phi_1(x, y, z) = x^2 + y^2 + z^2$$
$$\Phi_2(x, y, z) = x + 2y + 2z$$

Find the following at the point (3, 4, 12): **(a)** the maximum rate of increase of Φ_1; **(b)** the maximum rate of increase of Φ_2; and **(c)** the rate of increase of Φ_1 along the direction of the maximum rate of increase of Φ_2.

Ans. **(a)** 26; **(b)** 3; **(c)** $23\frac{1}{3}$.

D5.3. Find the Laplacians of the following functions: **(a)** x^2yz^3; **(b)** $(1/r) \sin \phi$ in cylindrical coordinates; and **(c)** $r^2 \cos \theta$ in spherical coordinates.

Ans. **(a)** $2yz^3 + 6x^2yz$; **(b)** 0; **(c)** $4 \cos \theta$.

5.2 POTENTIAL FUNCTIONS FOR STATIC FIELDS

Potential difference

As already pointed out in the preceding section, Eq. (5.13) reduces to

$$\boxed{\mathbf{E} = -\nabla\Phi} \tag{5.29}$$

for the static field case. We observe from (5.29) that the potential function Φ then is such that the electric field lines are orthogonal to the equipotential surfaces, that is, to the surfaces on which the potential remains constant, as shown in Fig. 5.2. If we consider two such equipotential surfaces corresponding to

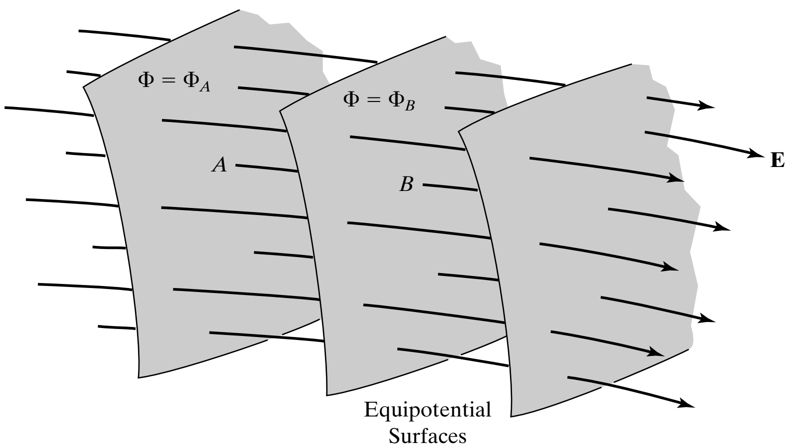

FIGURE 5.2

Set of equipotential surfaces in a region of static electric field.

$\Phi = \Phi_A$ and $\Phi = \Phi_B$, as shown in the figure, the potential difference $\Phi_A - \Phi_B$ is given, according to the definition of the gradient, by

$$\begin{aligned}\Phi_A - \Phi_B &= \int_B^A d\Phi = \int_B^A \nabla\Phi \cdot d\mathbf{l} \\ &= -\int_A^B \nabla\Phi \cdot d\mathbf{l}\end{aligned} \tag{5.30}$$

Using (5.29), we obtain

$$\boxed{\Phi_A - \Phi_B = \int_A^B \mathbf{E} \cdot d\mathbf{l}} \tag{5.31}$$

We now recall from Section 2.1 that $\int_A^B \mathbf{E} \cdot d\mathbf{l}$ is the voltage between points A and B. Thus, the potential difference in the static field case has the same meaning as the voltage. The reason for the minus sign in (5.13) and hence in (5.29) is now evident, since without it the voltage between A and B would be the negative of the potential difference between A and B.

Potential difference versus voltage

Before proceeding further, we recall that the voltage between two points A and B in a time-varying electric field is in general dependent on the path followed from A to B to evaluate $\int_A^B \mathbf{E} \cdot d\mathbf{l}$, since, according to Faraday's law,

$$\oint_C \mathbf{E} \cdot d\mathbf{l} = -\frac{d}{dt}\int_S \mathbf{B} \cdot d\mathbf{S}$$

is not in general equal to zero. On the other hand, the potential difference (or voltage) between two points A and B in a static electric field is independent of the path followed from A to B to evaluate $\int_A^B \mathbf{E} \cdot d\mathbf{l}$, since, for static fields,

$$\oint_C \mathbf{E} \cdot d\mathbf{l} = 0$$

Thus, the potential difference (or voltage) between two points in a static electric field has a unique value. Since the potential difference and voltage have the same meaning for static fields, we shall hereafter replace Φ in (5.29) by V, thereby writing

$$\boxed{\mathbf{E} = -\nabla V} \tag{5.32}$$

Electric potential due to a point charge

Let us now consider the electric field of a point charge and investigate the electric potential due to the point charge. To do this, we recall that the electric field intensity due to a point charge Q is directed radially away from the point charge and its magnitude is $Q/4\pi\varepsilon R^2$, where R is the radial distance from the point charge. Since the equipotential surfaces are everywhere orthogonal to the

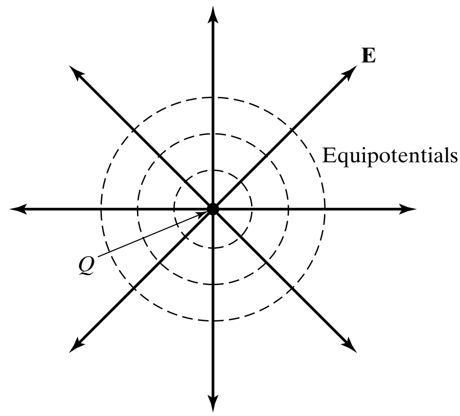

FIGURE 5.3

Cross-sectional view of equipotential surfaces and electric field lines for a point charge.

field lines, it then follows that they are spherical surfaces centered at the point charge, as shown by the cross-sectional view in Fig. 5.3. If we now consider two equipotential surfaces of radii R and $R + dR$, the potential drop from the surface of radius R to the surface of radius $R + dR$ is $(Q/4\pi\varepsilon R^2)\,dR$ or the incremental potential rise dV is given by

$$\begin{aligned} dV &= -\frac{Q}{4\pi\varepsilon R^2}dR \\ &= d\left(\frac{Q}{4\pi\varepsilon R} + C\right) \end{aligned} \tag{5.33}$$

where C is a constant. Thus,

$$V(R) = \frac{Q}{4\pi\varepsilon R} + C \tag{5.34}$$

Since the potential difference between two points does not depend on the value of C, we can choose C such that V is zero at some arbitrary reference point. Here we can conveniently set C equal to zero by noting that it is equal to $V(\infty)$ and by choosing $R = \infty$ for the reference point. Thus, we obtain the electric potential due to a point charge Q to be

$$\boxed{V = \frac{Q}{4\pi\varepsilon R}} \tag{5.35}$$

We note that the potential drops off inversely with the radial distance away from the point charge.

Equation (5.35) is often the starting point for the computation of the potential field due to static charge distributions and the subsequent determination of the electric field by using (5.32). We shall illustrate this by considering the case of the electric dipole in the following example.

Example 5.2 Electric field of a static electric dipole via the potential due to the dipole

Electric dipole

As we have learned in Section 4.2, the electric dipole consists of two equal and opposite point charges. Let us consider a static electric dipole consisting of point charges Q and $-Q$ situated on the z-axis at $z = d/2$ and $z = -d/2$, respectively, as shown in Fig. 5.4(a) and find the potential and hence the electric field at a point P far from the dipole.

First, we note that in view of the symmetry associated with the dipole around the z-axis, it is convenient to use the spherical coordinate system. Denoting the distance from the point charge Q to P to be r_1 and the distance from the point charge $-Q$ to P to be r_2, we write the expression for the electric potential at P due to the electric dipole as

$$V = \frac{Q}{4\pi\varepsilon r_1} + \frac{-Q}{4\pi\varepsilon r_2} = \frac{Q}{4\pi\varepsilon}\left(\frac{1}{r_1} - \frac{1}{r_2}\right)$$

For a point P far from the dipole, that is, for $r \gg d$, the lines drawn from the two charges to the point are almost parallel. Hence,

$$r_1 \approx r - \frac{d}{2}\cos\theta$$

$$r_2 \approx r + \frac{d}{2}\cos\theta$$

and

$$\frac{1}{r_1} - \frac{1}{r_2} = \frac{r_2 - r_1}{r_1 r_2} \approx \frac{d\cos\theta}{r^2}$$

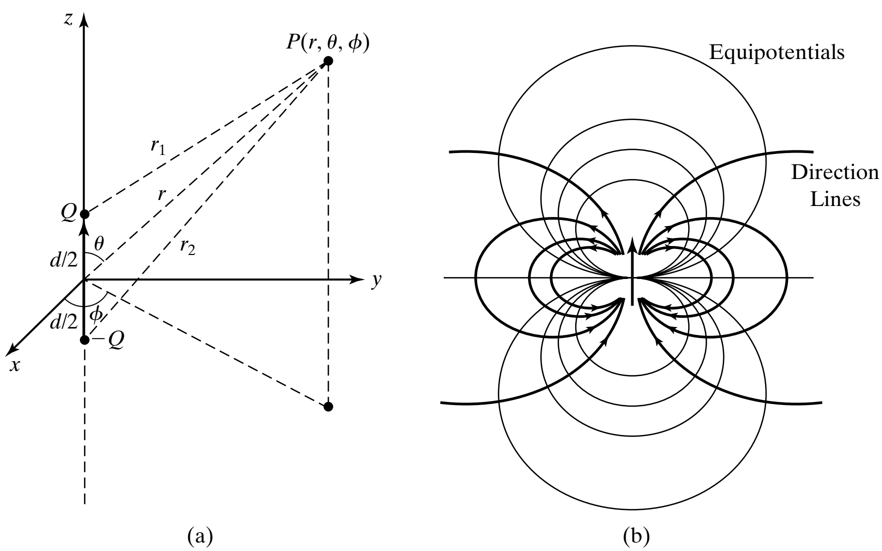

FIGURE 5.4

(a) Geometry pertinent to the determination of the electric field due to an electric dipole. (b) Cross sections of equipotential surfaces and direction lines of the electric field for the electric dipole.

so that

$$V \approx \frac{Qd\cos\theta}{4\pi\varepsilon r^2} = \frac{\mathbf{p}\cdot\mathbf{a}_r}{4\pi\varepsilon r^2} \tag{5.36}$$

where $\mathbf{p} = Qd\mathbf{a}_z$ is the dipole moment of the electric dipole. Thus, the potential field of the electric dipole drops off inversely with the square of the distance from the dipole. Proceeding further, we obtain the electric field intensity due to the dipole to be

$$\begin{aligned}\mathbf{E} = -\nabla V &= -\frac{\partial}{\partial r}\left(\frac{Qd\cos\theta}{4\pi\varepsilon r^2}\right)\mathbf{a}_r - \frac{1}{r}\frac{\partial}{\partial\theta}\left(\frac{Qd\cos\theta}{4\pi\varepsilon r^2}\right)\mathbf{a}_\theta \\ &= \frac{Qd}{4\pi\varepsilon r^3}(2\cos\theta\,\mathbf{a}_r + \sin\theta\,\mathbf{a}_\theta)\end{aligned} \tag{5.37}$$

Equation (5.36) shows that the equipotential surfaces are given by $r^2\sec\theta =$ constant, whereas from (5.37), it can be shown that the direction lines of the electric field are given by $r\operatorname{cosec}^2\theta =$ constant and $\phi =$ constant. These are shown sketched in Fig. 5.4(b). Alternative to using the equation for the direction lines, they can be sketched by recognizing that (1) they must originate from the positive charge and end on the negative charge and (2) they must be everywhere perpendicular to the equipotential surfaces.

Electro-cardiography

A technique in everyday life in which the potential field of an electric dipole is relevant is electrocardiography. This technique is based on the characterization of the electrical activity of the heart by using a dipole model.[2] The dipole moment, **p**, referred to in medical literature as the *electric force vector* or the *activity* of the heart, sets up an electric potential within the chest cavity and a characteristic pattern of equipotentials on the body surface. The potential differences between various points on the body are measured as a function of time and are used to deduce the temporal evolution of the dipole moment during the cardiac cycle, thereby monitoring changes in the electrical activity of the heart.

We shall now consider an example for illustrating a method of computer plotting of equipotentials when a closed form expression such as that for the electric dipole of Example 5.2 is not available.

Example 5.3 Computer plotting of equipotentials for a set of two point charges

Computer plotting of equipotentials

Let us consider two point charges $Q_1 = 8\pi\varepsilon_0$ C and $Q_2 = -4\pi\varepsilon_0$ C situated at $(-1, 0, 0)$ and $(1, 0, 0)$, respectively, as shown in Fig. 5.5. We wish to discuss the computer plotting of the equipotentials due to the two point charges.

First, we recognize that since the equipotential surfaces are surfaces of revolution about the axis of the two charges, it is sufficient to consider the equipotential lines in any plane containing the two charges. Here we shall consider the xz-plane. The equipotential lines are also symmetrical about the x-axis, and, hence, we shall plot them only on one

[2]See, for example, R. K. Hobbie, "The Electrocardiogram as an Example in Electrostatics," *American Journal of Physics*, June 1973, pp. 824–831.

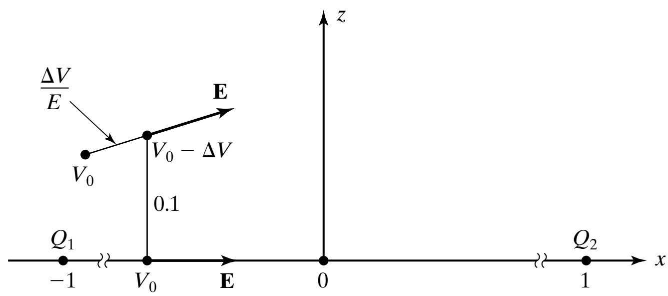

FIGURE 5.5

For illustrating the procedure for the computer plotting of equipotentials due to two point charges.

side of the x-axis and inside the rectangular region having corners at $(-4, 0)$, $(4, 0)(4, 5)$, and $(-4, 5)$.

As we go from Q_1 to Q_2 along the x-axis, the potential varies from $+\infty$ to $-\infty$ and is given by

$$\begin{aligned} V &= \frac{8\pi\varepsilon_0}{4\pi\varepsilon_0(1 + x)} - \frac{4\pi\varepsilon_0}{4\pi\varepsilon_0(1 - x)} \\ &= \frac{1 - 3x}{1 - x^2} \end{aligned}$$

The value of x lying between -1 and 1 for a given potential V_0 is then given by

$$V_0 = \frac{1 - 3x}{1 - x^2}$$

or

$$x = \begin{cases} \dfrac{3 - \sqrt{9 - 4V_0(1 - V_0)}}{2V_0} & \text{for} \quad V_0 \neq 0 \\ \dfrac{1}{3} & \text{for} \quad V_0 = 0 \end{cases}$$

We shall begin the equipotential line at this value of x on the x-axis for a given value of V_0. To plot the line, we make use of the property that the equipotential lines are orthogonal to the direction lines of **E** so that they are tangential to the unit vector $(E_z\mathbf{a}_x - E_x\mathbf{a}_z)/E$. We shall step along this unit vector by a small distance (chosen here to be 0.1), and if necessary, correct the position by repeatedly moving along the electric field until the potential is within a specified value (chosen here to be 0.001 V) of that for which the line is being plotted. To correct the position, we make use of the fact that $\nabla V = -\mathbf{E}$. Thus, the incremental distance required to be moved opposite to the electric field to increase the potential by ΔV is $\Delta V/E$, and, hence, the distances required to be moved opposite to the x- and z-directions are $(\Delta V/E)(E_x/E)$ and $(\Delta V/E)(E_z/E)$, respectively. The plotting of the line is terminated when the point goes out of the rectangular region.

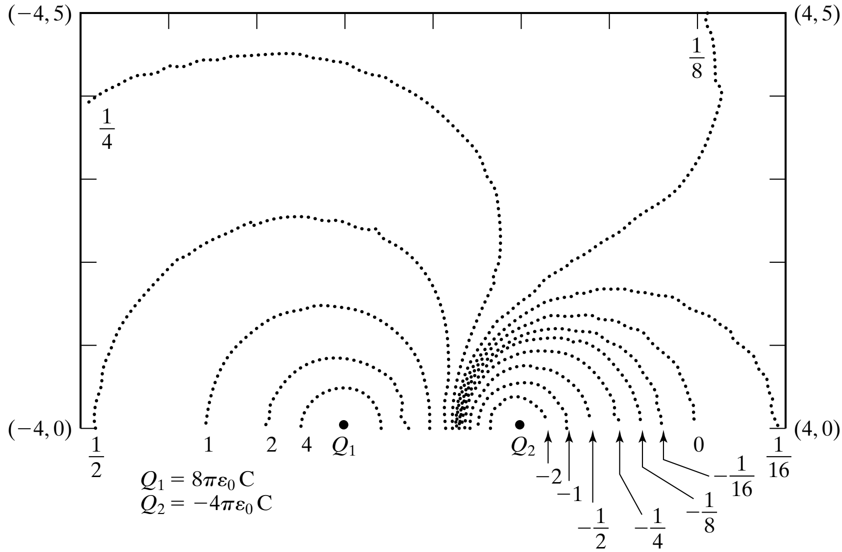

FIGURE 5.6

Personal computer-generated plot of equipotentials for the arrangement of two point charges of Fig. 5.5. The values of potentials are in volts.

The computer plot obtained from a run of a PC program that carries out this procedure for values of potentials ranging from −2 V to 4 V is shown in Fig. 5.6. It should, however, be pointed out that for a complete plot, those equipotential lines that surround both point charges should also be considered.

The computation of potential can be extended to continuous charge distributions by using superposition in conjunction with the expression for the potential due to a point charge, as in the case of electric field computation in Section 1.5. We shall illustrate by means of an example.

Example 5.4 Electric potential field of an infinitely long line charge

Potential due to a line charge

An infinitely long line charge of uniform density ρ_{L0} C/m is situated along the z-axis. It is desired to obtain the potential field due to this charge.

First, we divide the line into a number of infinitesimal segments each of length dz, as shown in Fig. 5.7, such that the charge $\rho_{L0}\,dz$ in each segment can be considered as a point charge. Let us consider a point P at a distance r from the z-axis, with the projection of P onto the z-axis being O. For the sake of generality, we consider the point P_0 at a distance r_0 from O along OP as the reference point for zero potential and write the potential dV at P due to the infinitesimal charge $\rho_{L0}\,dz$ at A as

$$\begin{aligned} dV &= \frac{\rho_{L0}\,dz}{4\pi\varepsilon_0(AP)} - \frac{\rho_{L0}\,dz}{4\pi\varepsilon_0(AP_0)} \\ &= \frac{\rho_{L0}\,dz}{4\pi\varepsilon_0\sqrt{r^2 + z^2}} - \frac{\rho_{L0}\,dz}{4\pi\varepsilon_0\sqrt{r_0^2 + z^2}} \end{aligned} \tag{5.38}$$

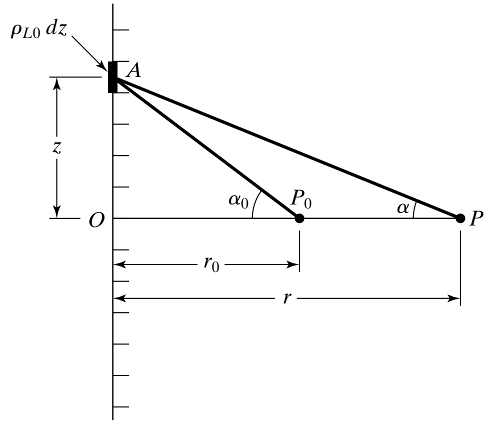

FIGURE 5.7

Geometry for the computation of the potential field of an infinitely long line charge of uniform density ρ_{L0} C/m.

We will, however, find later that we have to choose the reference point for zero potential at a finite value of r, in contrast to the case of the point charge for which the reference point can be chosen to be infinity. The potential V at P due to the entire line charge is now given by the integral of (5.38), where the integration is to be performed between the limits $z = -\infty$ and $z = \infty$. Thus,

$$\begin{aligned} V &= \int_{z=-\infty}^{\infty} dV = \int_{z=-\infty}^{\infty}\left(\frac{\rho_{L0}\,dz}{4\pi\varepsilon_0\sqrt{r^2 + z^2}} - \frac{\rho_{L0}\,dz}{4\pi\varepsilon_0\sqrt{r_0^2 + z^2}}\right) \\ &= \frac{\rho_{L0}}{2\pi\varepsilon_0}\int_{z=0}^{\infty}\left(\frac{dz}{\sqrt{r^2 + z^2}} - \frac{dz}{\sqrt{r_0^2 + z^2}}\right) \end{aligned} \tag{5.39}$$

Introducing $z = r\tan\alpha$ and $z = r_0\tan\alpha_0$ in the first and second terms, respectively, in the integrand on the right side of (5.39), we have

$$\begin{aligned} V &= \frac{\rho_{L0}}{2\pi\varepsilon_0}\left(\int_{\alpha=0}^{\pi/2}\sec\alpha\,d\alpha - \int_{\alpha_0=0}^{\pi/2}\sec\alpha_0\,d\alpha_0\right) \\ &= \frac{\rho_{L0}}{2\pi\varepsilon_0}\{[\ln(\sec\alpha + \tan\alpha)]_{\alpha=0}^{\pi/2} - [\ln(\sec\alpha_0 + \tan\alpha_0)]_{\alpha_0=0}^{\pi/2}\} \\ &= \frac{\rho_{L0}}{2\pi\varepsilon_0}\left[\ln\frac{(\sqrt{r^2 + z^2} + z)r_0}{(\sqrt{r_0^2 + z^2} + z)r}\right]_{z=0}^{\infty} \\ &= -\frac{\rho_{L0}}{2\pi\varepsilon_0}\ln\frac{r}{r_0} \end{aligned} \tag{5.40}$$

In view of the cylindrical symmetry about the line charge, (5.40) is the general expression in cylindrical coordinates for the potential field of the infinitely long line charge of uniform density. It can be seen from (5.40) that a choice of $r_0 = \infty$ is not a good choice, since then the potential would be infinity at all points. The difficulty lies in the fact that infinity plus a finite number is still infinity. We also note from (5.40) that the equipotential surfaces are $\ln r/r_0$ = constant or r = constant, that is, surfaces of cylinders with the line charge as their axis. The result of Example 2.6 shows that the electric field due to the line charge is directed radially away from the line charge. Thus, the direction lines of **E** and the equipotential surfaces are indeed orthogonal to each other.

Magnetic vector potential due to a current element

We shall now turn our attention to the magnetic vector potential for the static field case. Thus, let us consider a current element of length $d\mathbf{l}$ situated at the origin, as shown in Fig. 5.8, and carrying current I A. We shall obtain the magnetic vector potential due to this current element. To do this, we recall from Section 1.6 that the magnetic field due to it at a point $P(r, \theta, \phi)$ is given by

$$\mathbf{B} = \frac{\mu}{4\pi}\frac{I\,d\mathbf{l} \times \mathbf{a}_r}{r^2} \tag{5.41}$$

Expressing **B** as

$$\mathbf{B} = \frac{\mu}{4\pi} I\,d\mathbf{l} \times \left(-\nabla\frac{1}{r}\right) \tag{5.42}$$

and using the vector identity

$$\mathbf{A} \times \nabla\Phi = \Phi\nabla \times \mathbf{A} - \nabla \times \Phi\mathbf{A} \tag{5.43}$$

we obtain

$$\mathbf{B} = -\frac{\mu I}{4\pi r}\nabla \times d\mathbf{l} + \nabla \times \frac{\mu I\,d\mathbf{l}}{4\pi r} \tag{5.44}$$

Since $d\mathbf{l}$ is a constant, $\nabla \times d\mathbf{l} = \mathbf{0}$, and (5.44) reduces to

$$\mathbf{B} = \nabla \times \frac{\mu I d\mathbf{l}}{4\pi r} \tag{5.45}$$

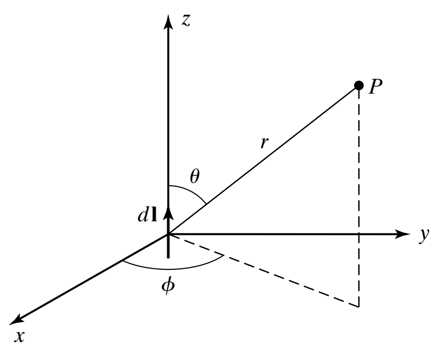

FIGURE 5.8

For finding the magnetic vector potential due to a current element.

Comparing (5.45) with (5.1), we see that the magnetic vector potential due to the current element situated at the origin is given by

$$\mathbf{A} = \frac{\mu I\, d\mathbf{l}}{4\pi r} \tag{5.46}$$

It follows from (5.46) that for a current element $I\, d\mathbf{l}$ situated at an arbitrary point, the magnetic vector potential is given by

$$\boxed{\mathbf{A} = \frac{\mu I\, d\mathbf{l}}{4\pi R}} \tag{5.47}$$

where R is the distance from the current element. Thus, it has a magnitude inversely proportional to the radial distance from the element (similar to the inverse distance dependence of the electric scalar potential due to a point charge) and direction parallel to the element. We shall make use of this result in Section 10.1.

K5.2. Potential difference; Potential due to a point charge; Computation of potential due to charge distributions; Electric dipole; Plotting of equipotential lines; Magnetic vector potential due to a current element.

D5.4. In a region of static electric field $\mathbf{E} = yz\mathbf{a}_x + zx\mathbf{a}_y + xy\mathbf{a}_z$, find the potential difference $V_A - V_B$ for each of the following pairs of points: **(a)** $A(2, 1, 1)$ and $B(1, 4, 0.5)$; **(b)** $A(2, 2, 2)$ and $B(1, 1, 1)$; and **(c)** $A(5, 1, 0.2)$ and $B(1, 2, 3)$.

Ans. **(a)** 0 V; **(b)** −7 V; **(c)** 5 V.

D5.5. Three point charges are located as follows: $30\pi\varepsilon_0$ C at (3, 4, 0), $10\pi\varepsilon_0$ C at (3, −4, 0), and $-40\pi\varepsilon_0$ C at (−5, 0, 0)). Find the following: **(a)** the potential at the point (0, 0, 3.2); **(b)** the coordinate x to three decimal places of the point on the x-axis at which the potential is a maximum; and **(c)** the potential at the point found in **(b)**.

Ans. **(a)** 0 V; **(b)** 3.872 m; **(c)** 1.3155 V.

D5.6. For each of the following arrangements of point charges, find the first significant term in the expression for the electric potential at distances far from the origin ($r \gg d$): **(a)** Q at $(0, 0, d)$, $2Q$ at $(0, 0, 0)$, and Q at $(0, 0, -d)$ and **(b)** Q at $(0, 0, d)$, $-2Q$ at $(0, 0, 0)$, and Q at $(0, 0, -d)$.

Ans. **(a)** $Q/\pi\varepsilon_0 r$; **(b)** $(Qd^2/4\pi\varepsilon_0 r^3)(3\cos^2\theta - 1)$.

5.3 POISSON'S AND LAPLACE'S EQUATIONS

Poisson's equation

In Section 5.2, we introduced the static electric potential as related to the static electric field in the manner

$$\boxed{\mathbf{E} = -\nabla V} \tag{5.48}$$

Substituting (5.48) into Maxwell's divergence equation for $\mathbf{D}$ given by

$$\nabla \cdot \mathbf{D} = \rho \tag{5.49}$$

we obtain

$$-\mathbf{\nabla} \cdot \varepsilon \mathbf{\nabla} V = \rho \tag{5.50}$$

where ε is the permittivity of the medium. Using the vector identity

$$\mathbf{\nabla} \cdot \Phi \mathbf{A} = \Phi \mathbf{\nabla} \cdot \mathbf{A} + \mathbf{A} \cdot \mathbf{\nabla} \Phi \tag{5.51}$$

we can write (5.50) as

$$\varepsilon \mathbf{\nabla} \cdot \mathbf{\nabla} V + \mathbf{\nabla} \varepsilon \cdot \mathbf{\nabla} V = -\rho$$

or

$$\boxed{\varepsilon \nabla^2 V + \mathbf{\nabla} \varepsilon \cdot \mathbf{\nabla} V = -\rho} \tag{5.52}$$

If we assume ε to be uniform in the region of interest, then $\mathbf{\nabla}\varepsilon = \mathbf{0}$ and (5.52) becomes

$$\boxed{\nabla^2 V = \frac{-\rho}{\varepsilon}} \tag{5.53}$$

This equation is known as Poisson's equation. It governs the relationship between the volume charge density ρ in a region of uniform permittivity ε to the electric scalar potential V in that region. Note that (5.53) also follows from (5.25) for $\partial/\partial t = 0$ and $\Phi = V$. In Cartesian coordinates, (5.53) becomes

$$\frac{\partial^2 V}{\partial x^2} + \frac{\partial^2 V}{\partial y^2} + \frac{\partial^2 V}{\partial z^2} = -\frac{\rho}{\varepsilon} \tag{5.54}$$

which is a three-dimensional, second-order partial differential equation. For the one-dimensional case in which V varies with x only, $\partial^2 V/\partial y^2$ and $\partial^2 V/\partial z^2$ are both equal to zero, and (5.54) reduces to

$$\boxed{\frac{\partial^2 V}{\partial x^2} = \frac{d^2 V}{dx^2} = -\frac{\rho}{\varepsilon}} \tag{5.55}$$

We shall illustrate the application of (5.55) by means of an example.

Example 5.5 Solution of Poisson's equation for a *p–n* junction semiconductor

p-n junction semiconductor

Let us consider the space charge layer in a *p-n* junction semiconductor with zero bias, as shown in Fig. 5.9(a), in which the region $x < 0$ is doped *p*-type and the region $x > 0$ is doped *n*-type. To review briefly the formation of the space charge layer, we note that since the density of the holes on the *p* side is larger than that on the *n* side, there is a tendency for the holes to diffuse to the *n* side and recombine with the electrons. Similarly, there is a tendency for the electrons on the *n* side to diffuse to the *p* side and recombine with the holes. The diffusion of holes leaves behind negatively charged acceptor atoms, and the diffusion of electrons leaves behind positively charged donor atoms. Since these

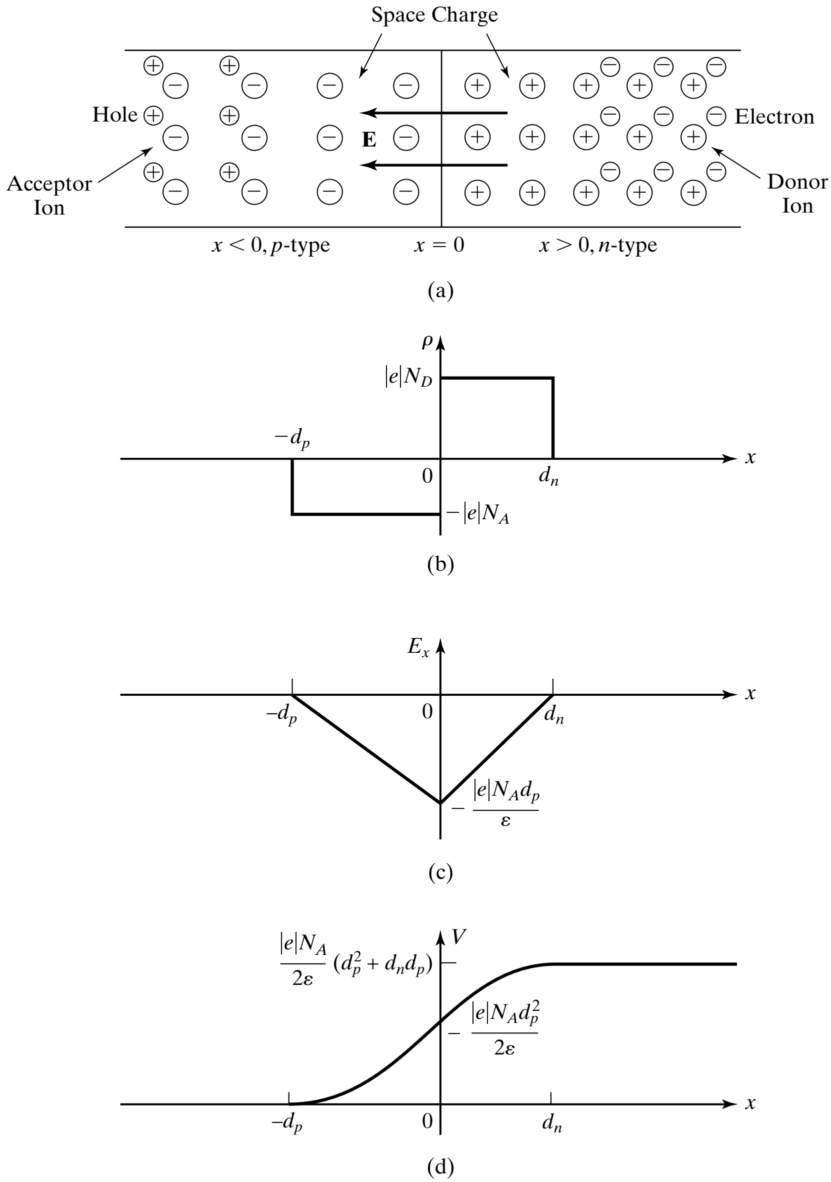

FIGURE 5.9

For illustrating the application of Poisson's equation for the determination of the potential distribution for a *p-n* junction semiconductor.

acceptor and donor atoms are immobile, a space charge layer, also known as the *depletion layer*, is formed in the region of the junction, with negative charges on the *p* side and positive charges on the *n* side. This space charge gives rise to an electric field directed from the *n* side of the junction to the *p* side so that it opposes diffusion of the mobile carriers across the junction, thereby resulting in an equilibrium. For simplicity, let us consider an abrupt junction, that is, a junction in which the impurity concentration is constant on either side of the junction. Let N_A and N_D be the acceptor and donor ion concentrations, respectively, and d_p and d_n be the widths in the p and n regions, respectively, of the depletion layer. The space charge density ρ is then given by

$$\rho = \begin{cases} -|e|N_A & \text{for} \quad -d_p < x < 0 \\ |e|N_D & \text{for} \quad 0 < x < d_n \end{cases} \tag{5.56}$$

as shown in Fig. 5.9(b), where $|e|$ is the magnitude of the electronic charge. Since the semiconductor is electrically neutral, the total acceptor charge must be equal to the total donor charge; that is,

$$|e|N_A d_p = |e|N_D d_n \tag{5.57}$$

We wish to find the potential distribution in the depletion layer and the depletion layer width in terms of the potential difference across the depletion layer and the acceptor and donor ion concentrations.

Substituting (5.56) into (5.55), we obtain the equation governing the potential distribution to be

$$\frac{d^2V}{dx^2} = \begin{cases} \dfrac{|e|N_A}{\varepsilon} & \text{for} \quad -d_p < x < 0 \\ -\dfrac{|e|N_D}{\varepsilon} & \text{for} \quad 0 < x < d_n \end{cases} \tag{5.58}$$

To solve (5.58) for V, we integrate it once and obtain

$$\frac{dV}{dx} = \begin{cases} \dfrac{|e|N_A}{\varepsilon}x + C_1 & \text{for} \quad -d_p < x < 0 \\ -\dfrac{|e|N_D}{\varepsilon}x + C_2 & \text{for} \quad 0 < x < d_n \end{cases}$$

where C_1 and C_2 are constants of integration. To evaluate C_1 and C_2, we note that since $\mathbf{E} = -\nabla V = -(\partial V/\partial x)\,\mathbf{a}_x$, $\partial V/\partial x$ is simply equal to $-E_x$. Since the electric field lines begin on the positive charges and end on the negative charges, and in view of (5.57), the field and, hence, $\partial V/\partial x$ must vanish at $x = -d_p$ and $x = d_n$, giving us

$$\frac{dV}{dx} = \begin{cases} \dfrac{|e|N_A}{\varepsilon}(x + d_p) & \text{for} \quad -d_p < x < 0 \\ -\dfrac{|e|N_D}{\varepsilon}(x - d_n) & \text{for} \quad 0 < x < d_n \end{cases} \tag{5.59}$$

The field intensity, that is, $-dV/dx$, may now be sketched as a function of x as shown in Fig. 5.9(c).

Proceeding further, we integrate (5.59) and obtain

$$V = \begin{cases} \dfrac{|e|N_A}{2\varepsilon}(x + d_p)^2 + C_3 & \text{for} \quad -d_p < x < 0 \\ -\dfrac{|e|N_D}{2\varepsilon}(x - d_n)^2 + C_4 & \text{for} \quad 0 < x < d_n \end{cases}$$

where C_3 and C_4 are constants of integration. To evaluate C_3 and C_4, we first set the potential at $x = -d_p$ arbitrarily equal to zero to obtain C_3 equal to zero. Then we make use of the condition that the potential be continuous at $x = 0$, since the discontinuity in dV/dx at $x = 0$ is finite, to obtain

$$\frac{|e|N_A}{2\varepsilon}d_p^2 = -\frac{|e|N_D}{2\varepsilon}d_n^2 + C_4$$

or

$$C_4 = \frac{|e|}{2\varepsilon}(N_A d_p^2 + N_D d_n^2)$$

Substituting this value for C_4 and setting C_3 equal to zero in the expression for V, we get the required solution

$$V = \begin{cases} \dfrac{|e|N_A}{2\varepsilon}(x + d_p)^2 & \text{for} \quad -d_p < x < 0 \\ -\dfrac{|e|N_D}{2\varepsilon}(x^2 - 2xd_n) + \dfrac{|e|N_A}{2\varepsilon}d_p^2 & \text{for} \quad 0 < x < d_n \end{cases} \tag{5.60}$$

The variation of potential with x as given by (5.60) is shown in Fig. 5.9(d).

We can proceed further and find the width $d = d_p + d_n$ of the depletion layer by setting $V(d_n)$ equal to the contact potential, V_0, that is, the potential difference across the depletion layer resulting from the electric field in the layer. Thus,

$$\begin{aligned} V_0 = V(d_n) &= \frac{|e|N_D}{2\varepsilon}d_n^2 + \frac{|e|N_A}{2\varepsilon}d_p^2 \\ &= \frac{|e|}{2\varepsilon}\frac{N_D(N_A + N_D)}{N_A + N_D}d_n^2 + \frac{|e|}{2\varepsilon}\frac{N_A(N_A + N_D)}{N_A + N_D}d_p^2 \\ &= \frac{|e|}{2\varepsilon}\frac{N_A N_D}{N_A + N_D}(d_n^2 + d_p^2 + 2d_n d_p) \\ &= \frac{|e|}{2\varepsilon}\frac{N_A N_D}{N_A + N_D}d^2 \end{aligned}$$

where we have made use of (5.57). Finally, we obtain the result that

$$d = \sqrt{\frac{2\varepsilon V_0}{|e|}\left(\frac{1}{N_A} + \frac{1}{N_D}\right)}$$

which tells us that the depletion layer width is smaller, the heavier the doping is. This property is used in tunnel diodes to achieve layer widths on the order of 10^{-6} cm by heavy doping as compared to widths on the order of 10^{-4} cm in ordinary p-n junctions.

We have just illustrated an example of the application of Poisson's equation involving the solution for the potential distribution for a given charge distribution. Poisson's equation is even more useful for the solution of problems in which the charge distribution is the quantity to be determined given the functional dependence of the charge density on the potential. We shall, however, proceed to the discussion of Laplace's equation.

Laplace's equation

If the charge density in a region is zero, then Poisson's equation (5.53) reduces to

$$\boxed{\nabla^2 V = 0} \tag{5.61}$$

This equation is known as *Laplace's equation*. It governs the behavior of the potential in a charge-free region characterized by uniform permittivity. In Cartesian coordinates, it is given by

$$\frac{\partial^2 V}{\partial x^2} + \frac{\partial^2 V}{\partial y^2} + \frac{\partial^2 V}{\partial z^2} = 0 \tag{5.62}$$

Laplace's equation is also satisfied by the potential in conductors under the steady-current condition. For the steady-current condition, $\partial\rho/\partial t = 0$, and the continuity equation given for the time-varying case by

$$\boldsymbol{\nabla} \cdot \mathbf{J}_c + \frac{\partial \rho}{\partial t} = 0$$

reduces to

$$\boldsymbol{\nabla} \cdot \mathbf{J}_c = 0 \tag{5.63}$$

Replacing $\mathbf{J}_c$ by $\sigma\mathbf{E} = -\sigma\boldsymbol{\nabla}V$, where σ is the conductivity of the conductor and assuming σ to be constant, we obtain

$$\boldsymbol{\nabla} \cdot \sigma\mathbf{E} = \sigma\boldsymbol{\nabla} \cdot \mathbf{E} = -\sigma\boldsymbol{\nabla} \cdot \boldsymbol{\nabla}V = -\sigma\nabla^2 V = 0$$

or

$$\nabla^2 V = 0$$

The problems to which Laplace's equation is applicable consist of finding the potential distribution in the region between two conductors, given the charge distribution on the surfaces of the conductors, or the potentials of the conductors, or a combination of the two. The procedure involves the solving of Laplace's equation subject to the boundary conditions on the surfaces of the conductors. We shall illustrate this by means of an example involving variation of V in one dimension.

Example 5.6 Solution of Laplace's equation for a parallel-plate capacitor

Parallel-plate arrangement, capacitance

Let us consider two infinite, plane, parallel, perfectly conducting plates occupying the planes $x = 0$ and $x = d$ and kept at potentials $V = 0$ and $V = V_0$, respectively, as shown by the cross-sectional view in Fig. 5.10, and find the solution for Laplace's equation in the region between the plates. The arrangement may be considered an idealization of a

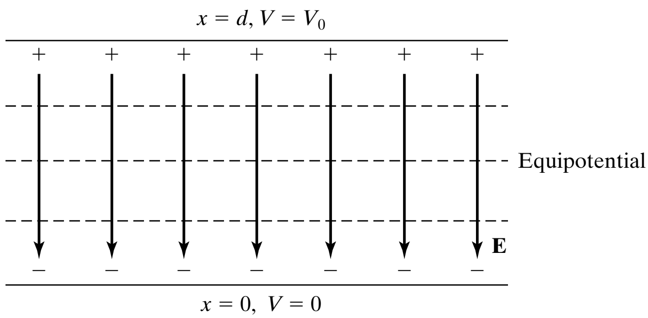

FIGURE 5.10

Cross-sectional view of parallel-plate capacitor for illustrating the solution of Laplace's equation in one dimension.

parallel-plate capacitor with its plates having dimensions very large compared to the spacing between them.

The potential is obviously a function of x only, and hence (5.62) reduces to

$$\frac{\partial^2 V}{\partial x^2} = \frac{\partial^2 V}{\partial x^2} = 0$$

Integrating this equation twice, we obtain

$$\boxed{V(x) = Ax + B} \tag{5.64}$$

where A and B are constants of integration. To determine the values of A and B, we make use of the boundary conditions for V; that is,

$$\begin{aligned} V &= 0 \quad \text{for} \quad x = 0 \\ V &= V_0 \quad \text{for} \quad x = d \end{aligned}$$

giving us

$$0 = A(0) + B \quad \text{or} \quad B = 0$$

$$V_0 = A(d) + B = Ad \quad \text{or} \quad A = \frac{V_0}{d}$$

Thus, the particular solution for the potential here is given by

$$\boxed{V = \frac{V_0}{d}x \quad \text{for} \quad 0 < x < d} \tag{5.65}$$

which tells us that the equipotentials are planes parallel to the conductors, as shown in Fig. 5.10.

Proceeding further, we obtain

$$\boxed{\mathbf{E} = -\nabla V = -\frac{\partial V}{\partial x}\mathbf{a}_x = -\frac{V_0}{d}\mathbf{a}_x \quad \text{for} \quad 0 < x < d} \tag{5.66}$$

This field is uniform and directed from the higher potential plate to the lower potential plate, as shown in Fig. 5.10. The surface charge densities on the two plates are given by

$$[\rho_S]_{x=0} = [\mathbf{D}]_{x=0} \cdot \mathbf{a}_x = -\frac{\varepsilon V_0}{d}\mathbf{a}_x \cdot \mathbf{a}_x = -\frac{\varepsilon V_0}{d}$$
$$[\rho_S]_{x=d} = [\mathbf{D}]_{x=d} \cdot (-\mathbf{a}_x) = -\frac{\varepsilon V_0}{d}\mathbf{a}_x \cdot (-\mathbf{a}_x) = \frac{\varepsilon V_0}{d}$$

The magnitude of the surface charge per unit area on either plate is

$$Q = |\rho_S|(1) = \frac{\varepsilon V_0}{d}$$

Finally, we can find the capacitance C per unit area of the plates, defined to be the ratio of Q to V_0. Thus,

$$\boxed{C = \frac{Q}{V_0} = \frac{\varepsilon}{d} \text{ per unit area of the plates}} \tag{5.67}$$

The units of capacitance are farads (F).

Parallel-plate arrangement, conductance

If the medium between the plates in Fig. 5.10 is a conductor, then the conduction current density is given by

$$\mathbf{J}_c = \sigma\mathbf{E} = -\frac{\sigma V_0}{d}\mathbf{a}_x$$

The conduction current from the higher potential plate to the lower potential plate per unit area of the plates is

$$I_c = |\mathbf{J}_c|(1) = \frac{\sigma V_0}{d}$$

The ratio of this current to the potential difference is the conductance G (reciprocal of resistance) per unit area of the plates. Thus,

$$\boxed{G = \frac{I_c}{V_0} = \frac{\sigma}{d} \text{ per unit area of the plates}} \tag{5.68}$$

The units of conductance are siemens (S).

Cylindrical and spherical capacitors

We have just illustrated the solution of Laplace's equation in one dimension by considering an example involving the variation of V with one Cartesian coordinate. In a similar manner, solutions for one-dimensional Laplace's equations involving variations of V with single coordinates in the other two coordinate systems can be obtained. Of particular interest are the case in which V is a function of the cylindrical coordinate r only, pertinent to the geometry of a capacitor made up of coaxial cylindrical conductors, and the case in which V is a

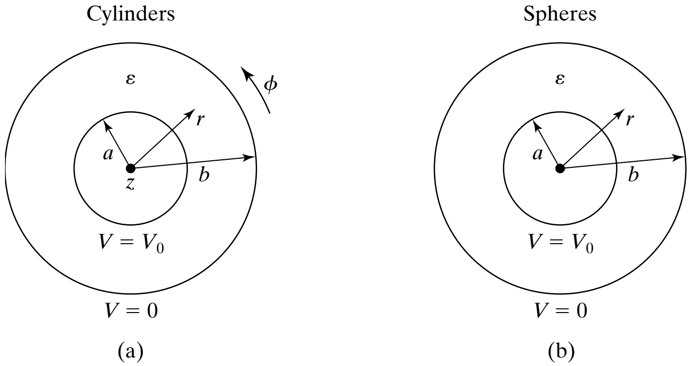

FIGURE 5.11

Cross-sectional views of capacitors made up of (a) coaxial cylindrical conductors and (b) concentric spherical conductors.

function of the spherical coordinate r only, pertinent to the geometry of a capacitor made up of concentric spherical conductors. These two geometries are shown in Figs. 5.11(a) and (b), respectively. The various steps in the solution of Laplace's equation and subsequent determination of capacitance for these two cases are summarized in Table 5.1, which also includes the parallel plane case of Fig. 5.10.

TABLE 5.1 Summary of Various Steps in the Solution of Laplace's Equation and Determination of Capacitance for Three One-Dimensional Cases

Geometry	Parallel planes	Coaxial cylinders	Concentric spheres
Figure	5.10	5.11(a)	5.11(b)
Boundary conditions	$\begin{cases} V = 0, & x = 0 \\ V = V_0, & x = d \end{cases}$	$V = V_0, \quad r = a$ $V = 0, \quad r = b$	$V = V_0, \quad r = a$ $V = 0, \quad r = b$
Laplace's equation	$\frac{\partial^2 V}{\partial x^2} = 0$	$\frac{1}{r}\frac{\partial}{\partial r}\left(r\frac{\partial V}{\partial r}\right) = 0$	$\frac{1}{r^2}\frac{\partial}{\partial r}\left(r^2\frac{\partial V}{\partial r}\right) = 0$
General solution	$V = Ax + B$	$V = A \ln r + B$	$V = \frac{A}{r} + B$
Particular solution	$V = V_0\frac{x}{d}$	$V = V_0\frac{\ln (r/b)}{\ln (a/b)}$	$V = V_0\frac{1/r - 1/b}{1/a - 1/b}$
Electric field	$-\frac{V_0}{d}\mathbf{a}_x$	$\frac{V_0}{r \ln (b/a)}\mathbf{a}_r$	$\frac{V_0}{r^2 (1/a - 1/b)}\mathbf{a}_r$
Surface charge densities	$\begin{cases} -\frac{\varepsilon V_0}{d}, & x = 0 \\ \frac{\varepsilon V_0}{d}, & x = d \end{cases}$	$\frac{\varepsilon V_0}{a \ln (b/a)}, \quad r = a$ $\frac{-\varepsilon V_0}{b \ln (b/a)}, \quad r = b$	$\frac{\varepsilon V_0}{a^2 (1/a - 1/b)}, \quad r = a$ $\frac{-\varepsilon V_0}{b^2 (1/a - 1/b)}, \quad r = b$
Capacitance	$\frac{\varepsilon}{d}$ per unit area	$\frac{2\pi\varepsilon}{\ln (b/a)}$ per unit length	$\frac{4\pi\varepsilon}{1/a - 1/b}$

K5.3. Poisson's equation; *p-n* junction; Laplace's equation in one dimension; Parallel-plate arrangement; Capacitance; Conductance; Cylindrical and spherical capacitors.

D5.7. The potential distribution in a simplified model of a vacuum diode consisting of cathode in the plane $x = 0$ and anode in the plane $x = d$ and held at a potential V_0 relative to the cathode is given by $V = V_0(x/d)^{4/3}$ for $0 < x < d$. Find the following: **(a)** V at $x = d/8$; **(b)** $\mathbf{E}$ at $x = d/8$; **(c)** ρ at $x = d/8$; and **(d)** ρ_S on the anode.

Ans. **(a)** $V_0/16$; **(b)** $-(2V_0/3d)\mathbf{a}_x$; **(c)** $-16\varepsilon_0 V_0/9d^2$; **(d)** $4\varepsilon_0 V_0/3d$.

D5.8. Find the following: **(a)** the spacing between the plates of a parallel-plate capacitor with a dielectric of $\varepsilon = 2.25\varepsilon_0$, and having capacitance per unit area equal to 1000 pF; **(b)** the ratio of the outer radius to the inner radius for a coaxial cylindrical capacitor with a dielectric of $\varepsilon = 2.25\varepsilon_0$, and having capacitance per unit length equal to 100 pF; and **(c)** the radius of an isolated spherical conductor in free space for which the capacitance is 10 pF.

Ans. **(a)** 1.99 cm; **(b)** 3.4903; **(c)** 9 cm.

5.4 CAPACITANCE, CONDUCTANCE, AND INDUCTANCE

In the previous section, we introduced the capacitance and conductance by considering the solution of Laplace's equation in one dimension. Specifically, we derived the expressions for the capacitance per unit area and the conductance per unit area of a parallel-plate arrangement, the capacitance per unit length of a coaxial cylindrical arrangement, and the capacitance of a concentric spherical arrangement.

Coaxial cylindrical arrangement

Let us now consider the three arrangements shown in Fig. 5.12, each of which is a cross-sectional view of a pair of infinitely long coaxial perfectly conducting cylinders with a material medium between them. In Fig. 5.12(a), the

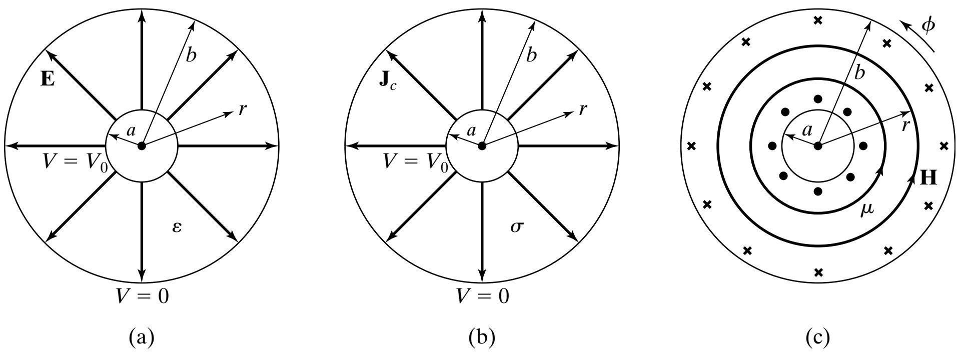

FIGURE 5.12

Cross sections of three arrangements, each consisting of two infinitely long, coaxial, perfectly conducting cylinders. The medium between the cylinders is a perfect dielectric for (a), a conductor for (b), and a magnetic material for (c).

material medium is a dielectric of uniform permittivity ε; in Fig. 5.12(b), it is a conductor of uniform conductivity σ; and in Fig. 5.12(c), it is a magnetic material of uniform permeability μ. In (a) and (b), a potential difference of V_0 is applied between the conductors, whereas in (c), a current I flows with uniform density in the $+z$-direction on the inner cylinder and returns with uniform density in the $-z$-direction on the outer cylinder.

Capacitance per unit length, $\mathscr{C}$

We know from the discussion in Section 5.3 that the arrangement of Fig. 5.12(a) is that of a coaxial cylindrical capacitor and from Table 5.1 that its capacitance (C) per unit length, defined as the magnitude of the charge per unit length on either conductor to the potential difference between the conductors, is given by

$$\boxed{\mathscr{C} = \frac{C}{l} = \frac{2\pi\varepsilon}{\ln(b/a)}} \tag{5.69}$$

the units of C being farads (F) and, hence, those of $\mathscr{C}$ being F/m.

Conductance per unit length, $\mathscr{G}$

Just as in the case of the parallel-plate arrangement of Example 5.7, replacing the dielectric in Fig. 6.4(a) by a conductor as in Fig. 5.12(b) would result in a conduction current of density

$$\mathbf{J}_c = \sigma\mathbf{E} = \frac{\sigma V_0}{r\ln(b/a)}\mathbf{a}_r$$

in the medium and, hence, a current per unit length

$$\begin{aligned} I_c &= \int_{\phi=0}^{2\pi} \mathbf{J}_c \cdot r\,d\phi\,\mathbf{a}_r = \int_{\phi=0}^{2\pi} \frac{\sigma V_0}{r\ln(b/a)} r\,d\phi \\ &= \frac{2\pi\sigma V_0}{\ln(b/a)} \end{aligned}$$

from the inner cylinder to the outer cylinder. Thus, the ratio of the current per unit length from the inner to the outer cylinder to the potential difference between the cylinders, that is, the conductance (G) per unit length of the arrangement, is given by

$$\boxed{\mathscr{G} = \frac{G}{l} = \frac{2\pi\sigma}{\ln(b/a)}} \tag{5.70}$$

the units of G being siemens (S) and, hence, those of $\mathscr{G}$ being S/m.

Inductance per unit length, $\mathscr{L}$

Turning now to Fig. 5.12(c), we know from the application of Ampere's circuital law in integral form that the current flow on the cylinders results in a magnetic field between the cylinders as given by

$$\mathbf{H} = \frac{I}{2\pi r}\mathbf{a}_\phi \quad \text{for} \qquad a < r < b$$

The magnetic flux density is then given by

$$\mathbf{B} = \mu\mathbf{H} = \frac{\mu I}{2\pi r}\mathbf{a}_\phi \quad \text{for} \qquad a < r < b$$

The magnetic flux linking the current per unit length of the conductors is

$$\begin{aligned} \psi &= \int_{r=a}^{b} \mathbf{B} \cdot dr\, \mathbf{a}_\phi \\ &= \int_{r=a}^{b} \frac{\mu I}{2\pi r}\, dr \\ &= \frac{\mu I}{2\pi} \ln \frac{b}{a} \end{aligned}$$

We now define the inductance (L) per unit length of the arrangement to be the ratio of the magnetic flux linking the current per unit length of the arrangement to the current. Thus,

$$\boxed{\mathscr{L} = \frac{L}{l} = \frac{\mu}{2\pi} \ln \frac{b}{a}} \tag{5.71}$$

The units of L are henrys (H) and, hence, those of $\mathscr{L}$ are H/m.

An examination of (5.69), (5.70), and (5.71) reveals that

$$\boxed{\frac{\mathscr{G}}{\mathscr{C}} = \frac{\sigma}{\varepsilon}} \tag{5.72}$$

and

$$\boxed{\mathscr{L}\mathscr{C} = \mu\varepsilon} \tag{5.73}$$

Thus, only one of the three parameters $\mathscr{C}$, $\mathscr{G}$, and $\mathscr{L}$ is independent, with the other two obtainable from it and the material parameters. Although this result is deduced here for the coaxial cylindrical arrangement, it is a general result valid for all arrangements involving two infinitely long, parallel perfect conductors embedded in a homogeneous medium (a medium of uniform material parameters). Expressions for the three quantities $\mathscr{C}$, $\mathscr{G}$, and $\mathscr{L}$ are listed in Table 5.2 for some common configurations of conductors having cross-sectional views shown in Fig. 5.13. The coaxial cylindrical arrangement is repeated for the sake of completion.

TABLE 5.2 Conductance, Capacitance, and Inductance per Unit Length for Some Structures Consisting of Infinitely Long Conductors Having the Cross Sections Shown in Fig. 5.13

Description	Capacitance per unit length, $\mathscr{C}$	Conductance per unit length, $\mathscr{G}$	Inductance per unit length, $\mathscr{L}$
Parallel-plane conductors, Fig. 5.13 (a)	$\varepsilon \dfrac{w}{d}$	$\sigma \dfrac{w}{d}$	$\mu \dfrac{d}{w}$
Coaxial cylindrical conductors, Fig. 5.13 (b)	$\dfrac{2\pi\varepsilon}{\ln(b/a)}$	$\dfrac{2\pi\sigma}{\ln(b/a)}$	$\dfrac{\mu}{2\pi} \ln \dfrac{b}{a}$
Parallel cylindrical wires, Fig. 5.13 (c)	$\dfrac{\pi\varepsilon}{\cosh^{-1}(d/a)}$	$\dfrac{\pi\sigma}{\cosh^{-1}(d/a)}$	$\dfrac{\mu}{\pi} \cosh^{-1} \dfrac{d}{a}$
Eccentric inner conductor, Fig. 5.13 (d)	$\dfrac{2\pi\varepsilon}{\cosh^{-1}\left(\dfrac{a^2+b^2-d^2}{2ab}\right)}$	$\dfrac{2\pi\sigma}{\cosh^{-1}\left(\dfrac{a^2+b^2-d^2}{2ab}\right)}$	$\dfrac{\mu}{2\pi} \cosh^{-1}\left(\dfrac{a^2+b^2+d^2}{2ab}\right)$
Shielded parallel cylindrical wires, Fig. 5.13 (e)	$\dfrac{\pi\varepsilon}{\ln \dfrac{d(b^2-d^2/4)}{a(b^2+d^2/4)}}$	$\dfrac{\pi\sigma}{\ln \dfrac{d(b^2-d^2/4)}{a(b^2+d^2/4)}}$	$\dfrac{\mu}{\pi} \ln \dfrac{d(b^2-d^2/4)}{a(b^2+d^2/4)}$

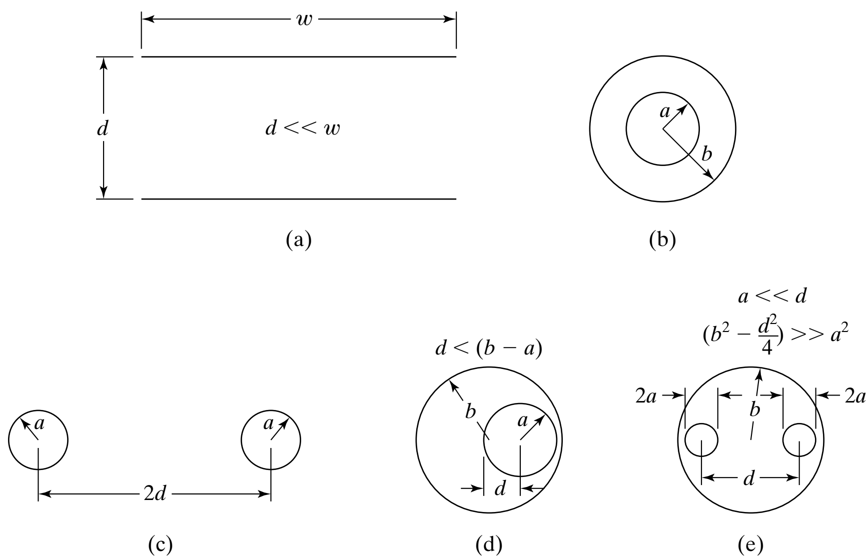

FIGURE 5.13
Cross sections of some common configurations of parallel, infinitely long conductors.

Example 5.7 Capacitance, conductance, and inductance per unit length for a parallel-wire line

$\mathscr{C}$, $\mathscr{G}$ and $\mathscr{L}$ of parallel-cylindrical wire arrangement

It is desired to obtain the capacitance, conductance, and inductance per unit length of the parallel-cylindrical wire arrangement of Fig. 5.13(c).

In view of (5.72) and (5.73), it is sufficient to find one of the three quantities. Hence, we choose to find the capacitance per unit length. Here we shall do this by considering the electric potential field of two parallel, infinitely long, straight-line charges of equal and opposite uniform charge densities and showing that the equipotential surfaces are cylinders having their axes parallel to the line charges. By placing conductors in two equipotential surfaces, thereby forming a parallel-wire line, we shall obtain the expression for the capacitance per unit length of the line.

Let us first consider an infinitely long, straight-line charge of uniform density ρ_{L0} C/m situated along the z-axis, as shown in Fig. 5.14(a), and obtain the electric potential due to the line charge. The symmetry associated with the problem indicates that the potential is dependent on the cylindrical coordinate r. Thus, we have

$$\begin{aligned} \nabla^2 V &= \frac{1}{r}\frac{\partial}{\partial r}\left(r\frac{\partial V}{\partial r}\right) = 0 \qquad \text{for} \quad r \neq 0 \\ V &= A \ln r + B \end{aligned} \tag{5.74}$$

where A and B are constants to be determined. We can arbitrarily set the potential to be zero at a reference value $r = r_0$, giving us $B = -A \ln r_0$ and

$$V = A \ln r - A \ln r_0 = A \ln \frac{r}{r_0} \tag{5.75}$$

To evaluate the arbitrary constant A in (5.75), we find that the electric-field intensity due to the line charge is given by

$$\mathbf{E} = -\nabla V = -\frac{\partial V}{\partial r}\mathbf{a}_r = -\frac{A}{r}\mathbf{a}_r$$

The electric field is thus directed radial to the line charge. Let us now consider a cylindrical box of radius r and length l coaxial with the line charge, as shown in Fig. 5.14(a), and apply Gauss' law for the electric field in integral form to the surface of the box. For the cylindrical surface,

$$\int \mathbf{D} \cdot d\mathbf{S} = -\frac{\varepsilon A}{r}(2\pi r l)$$

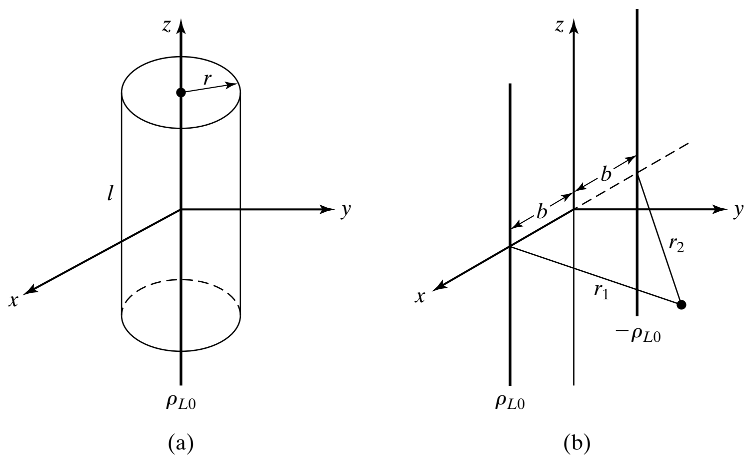

FIGURE 5.14

(a) Infinitely long line charge of uniform density along the z-axis. (b) Pair of parallel, infinitely long line charges of equal and opposite uniform densities.

For the top and bottom surfaces, $\int \mathbf{D} \cdot d\mathbf{S} = 0$, since the field is parallel to the surfaces. The charge enclosed by the box is $\rho_{L0}l$. Thus, we have

$$-\frac{\varepsilon A}{r}(2\pi r l) = \rho_{L0} l \qquad \text{or} \qquad A = -\frac{\rho_{L0}}{2\pi\varepsilon}$$

Substituting this result in (5.75), we obtain the potential field due to the line charge to be

$$V = -\frac{\rho_{L0}}{2\pi\varepsilon}\ln\frac{r}{r_0} = \frac{\rho_{L0}}{2\pi\varepsilon}\ln\frac{r_0}{r} \tag{5.76}$$

which is consistent with (5.40).

Let us now consider two infinitely long, straight-line charges of equal and opposite uniform charge densities ρ_{L0} C/m and $-\rho_{L0}$ C/m, parallel to the z-axis and passing through $x = b$ and $x = -b$, respectively, as shown in Fig. 5.14(b). Applying superposition and using (5.76), we write the potential due to the two line charges as

$$V = \frac{\rho_{L0}}{2\pi\varepsilon}\ln\frac{r_{01}}{r_1} - \frac{\rho_{L0}}{2\pi\varepsilon}\ln\frac{r_{02}}{r_2}$$

where r_1 and r_2 are the distances of the point of interest from the line charges and r_{01} and r_{02} are the distances to the reference point at which the potential is zero. By choosing the reference point to be equidistant from the two line charges, that is, $r_{01} = r_{02}$, we get

$$V = \frac{\rho_{L0}}{2\pi\varepsilon}\ln\frac{r_2}{r_1} \tag{5.77}$$

From (5.77), we note that the equipotential surfaces for the potential field of the line-charge pair are given by

$$\frac{r_2}{r_1} = \text{constant, say, } k \tag{5.78}$$

where k lies between 0 and ∞. In terms of Cartesian coordinates, (5.78) can be written as

$$\frac{(x + b)^2 + y^2}{(x - b)^2 + y^2} = k^2$$

Rearranging, we obtain

$$x^2 - 2b\frac{k^2 + 1}{k^2 - 1}x + y^2 + b^2 = 0$$

or

$$\left(x - b\frac{k^2 + 1}{k^2 - 1}\right)^2 + y^2 = \left(b\frac{2k}{k^2 - 1}\right)^2$$

This equation represents cylinders having their axes along

$$x = b\frac{k^2 + 1}{k^2 - 1}, \qquad y = 0$$

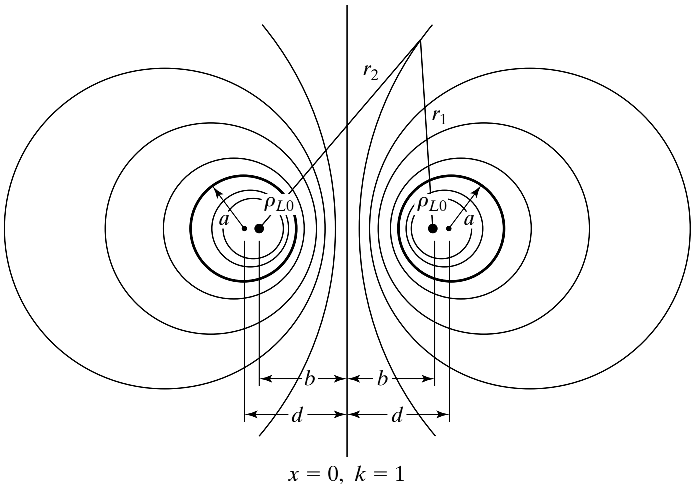

FIGURE 5.15

Cross sections of equipotential surfaces for the line charge pair of Fig 5.14(b). Thick circles represent a cross section of parallel-wire line.

and radii equal to $b[2k/(k^2 - 1)]$. The corresponding potentials are $(\rho_{L0}/2\pi\varepsilon)\ln k$. The cross sections of the equipotential surfaces are shown in Fig. 5.15.

We can now place perfectly conducting cylinders in any two equipotential surfaces without disturbing the field configuration, as shown, for example, by the thick circles in Fig. 5.15, thereby obtaining a parallel-wire line. Letting the distance between their centers be $2d$ and their radii be a, we have

$$\pm d = b\frac{k^2 + 1}{k^2 - 1}$$
$$a = b\frac{2k}{k^2 - 1}$$

Solving these two equations for k and accepting only those solutions lying between 0 and ∞, we obtain

$$k = \frac{d \pm \sqrt{d^2 - a^2}}{a}$$

The potentials of the right $(k > 1)$ and left $(k < 1)$ conductors are then given, respectively, by

$$V_+ = \frac{\rho_{L0}}{2\pi\varepsilon}\ln\frac{d + \sqrt{d^2 - a^2}}{a}$$
$$V_- = \frac{\rho_{L0}}{2\pi\varepsilon}\ln\frac{d - \sqrt{d^2 - a^2}}{a}$$
$$= -\frac{\rho_{L0}}{2\pi\varepsilon}\ln\frac{d + \sqrt{d^2 - a^2}}{a}$$

The potential difference between the two conductors is

$$V_0 = V_+ - V_- = \frac{\rho_{L0}}{\pi\varepsilon} \ln \frac{d + \sqrt{d^2 - a^2}}{a}$$

Finally, to find the capacitance, we note that since the electric field lines begin on the positive charge and end on the negative charge orthogonal to the equipotentials, the magnitude of the charge on either conductor, which produces the same field as the line-charge pair, must be the same as the line charge itself. Thus, considering unit length of the line, we obtain the capacitance per unit length of the parallel-wire line to be

$$\boxed{\begin{aligned} \mathscr{C} = \frac{\rho_{L0}}{V_0} &= \frac{\pi\varepsilon}{\ln\left[\left(d + \sqrt{d^2 - a^2}\right)/a\right]} \\ &= \frac{\pi\varepsilon}{\cosh^{-1}(d/a)} \end{aligned}} \tag{5.79}$$

and, hence, the expressions for $\mathscr{G}$ and $\mathscr{L}$, as given in Table 5.2.

Internal inductance

If the conductors in a given configuration are not perfect, then the currents flow in the volumes of the conductors instead of being confined to the surfaces. We then have to consider the magnetic field internal to the current distribution in addition to the magnetic field external to it. The inductance associated with the internal field is known as the *internal inductance* as compared to the *external inductance* associated with the external field. The expressions for the inductance per unit length given in Table 5.2 are for the external inductance. To obtain the internal inductance, we have to take into account the fact that different flux lines in the volume occupied by the current distribution link different partial amounts of the total current. We shall illustrate this by means of an example.

Example 5.8 Internal inductance per unit length of a solid cylindrical conductor

A current I A flows with uniform volume density $\mathbf{J} = J_0\mathbf{a}_z$ A/m^2 along an infinitely long, solid cylindrical conductor of radius a and returns with uniform surface density in the opposite direction along the surface of an infinitely long, perfectly conducting cylinder of radius $b\,(>a)$ and coaxial with the inner conductor. It is desired to find the internal inductance per unit length of the inner conductor.

The cross-sectional view of the conductor arrangement is shown in Fig. 5.16(a). From symmetry considerations, the magnetic field is entirely in the ϕ direction and independent of ϕ. Applying Ampère's circuital law to a circular contour of radius $r\,(<a)$, as shown in Fig. 5.16(a), we have

$$2\pi r H_\phi = \pi r^2 J_0$$

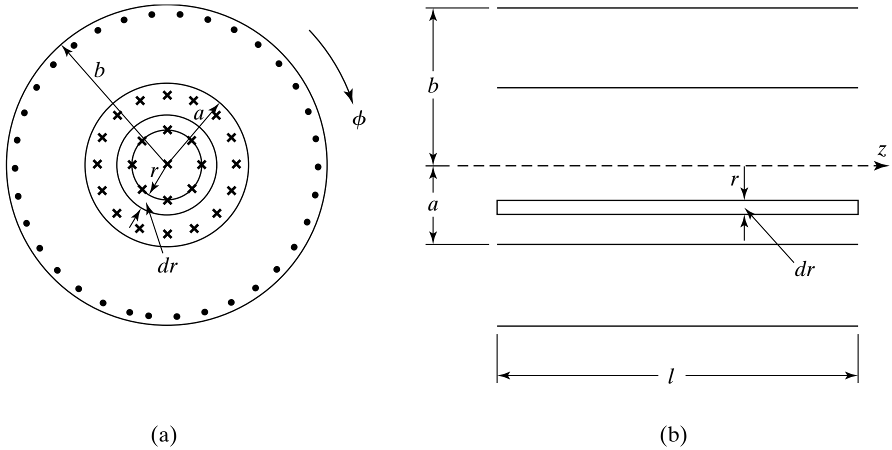

FIGURE 5.16

For evaluating the internal inductance per unit length associated with a volume current of uniform density along an infinitely long cylindrical conductor.

or

$$\mathbf{H} = H_\phi \mathbf{a}_\phi = \frac{J_0 r}{2}\mathbf{a}_\phi \qquad r < a$$

The corresponding magnetic flux density is given by

$$\mathbf{B} = \mu\mathbf{H} = \frac{\mu J_0 r}{2}\mathbf{a}_\phi \qquad r < a$$

where μ is the permeability of the conductor. Let us now consider a rectangle of infinitesimal width dr in the r-direction and length l in the z-direction at a distance r from the axis, as shown in Fig. 5.16(b). The magnetic flux $d\psi_i$ crossing this rectangular surface is given by

$$\begin{aligned} d\psi_i &= B_\phi \text{ (area of the rectangle)} \\ &= \frac{\mu J_0 r l\, dr}{2} \end{aligned}$$

where the subscript i denotes flux internal to the conductor. This flux surrounds only the current flowing within the radius r, as can be seen from Fig. 5.16(a). Let N be the fraction of the total current I linked by this flux. Then

$$\begin{aligned} N &= \frac{\text{current flowing within radius } r \ (< a)}{\text{total current } I} \\ &= \frac{J_0 \pi r^2}{J_0 \pi a^2} = \left(\frac{r}{a}\right)^2 \end{aligned}$$

The contribution from the flux $d\psi_i$ to the internal flux linkage associated with the current I is the product of N and the flux itself, that is, $N\,d\psi_i$. To obtain the internal flux linkage associated with I, we integrate $N\,d\psi_i$ between the limits $r = 0$ and $r = a$, taking into account the dependence of N on $d\psi_i$. Thus,

$$\psi_i = \int_{r=0}^{a} N\,d\psi_i = \int_{r=0}^{a} \left(\frac{r}{a}\right)^2 \frac{\mu J_0 l r}{2}\,dr = \frac{\mu J_0 l a^2}{8}$$

Finally, the required internal inductance per unit length is

$$\boxed{\mathscr{L}_i = \frac{\psi_i}{lI} = \frac{\mu J_0 a^2/8}{J_0 \pi a^2} = \frac{\mu}{8\pi}} \tag{5.80}$$

From the steps involved in the solution of Example 5.8, we observe that the general expression for the internal inductance is

$$\boxed{L_{\text{int}} = \frac{1}{I}\int_S N\,d\psi} \tag{5.81a}$$

where S is any surface through which the internal magnetic flux associated with I passes. We note that (5.81a) is also good for computing the external inductance since for external inductance, N is independent of $d\psi$. Hence,

$$L_{\text{ext}} = \frac{N}{I}\int_S d\psi = N\frac{\psi}{I} \tag{5.81b}$$

In (5.81b), the value of N is unity if I is a surface current, as in the arrangement of Fig. 5.12(c). On the other hand, for a filamentary wire wound on a core, N is equal to the number of turns of the winding, in which case ψ represents the flux through the core, that is, the flux crossing the surface formed by one turn, according to the same consideration as that in conjunction with the discussion of Faraday's law for an N-turn coil (see Fig. 2.13).

Mutual inductance

The discussion pertaining to inductance thus far has been concerned with *self-inductance*, that is, inductance associated with a current distribution by virtue of its own flux linking it. On the other hand, if we have two independent currents I_1 and I_2, we can talk of the flux due to one current linking the second current. This leads to the concept of *mutual inductance*. The mutual inductance denoted as L_{12} is defined as

$$\boxed{L_{12} = N_1\frac{\psi_{12}}{I_2}} \tag{5.82a}$$

where ψ_{12} is the magnetic flux produced by I_2 but linking one turn of the N_1-turn winding carrying current I_1. Similarly,

$$\boxed{L_{21} = N_2 \frac{\psi_{21}}{I_1}} \tag{5.82b}$$

where ψ_{21} is the magnetic flux produced by I_1 but linking one turn of the N_2-turn winding carrying current I_2. It can be shown that $L_{21} = L_{12}$. We shall now consider a simple example illustrating the computation of mutual inductance.

Example 5.9 Mutual inductance per unit length between a single wire and a two-wire telephone line

A single straight wire, infinitely long and carrying current I_1, lies below to the left and parallel to a two-wire telephone line carrying current I_2, as shown by the cross-sectional and plan views in Figs. 5.17(a) and (b), respectively. It is desired to obtain the mutual inductance between the single wire and the telephone line per unit length of the wires. The thickness of the telephone wire is assumed to be negligible.

Choosing a coordinate system with the axis of the single wire as the z-axis and applying Ampère's circuital law to a circular path around the single wire, we obtain the magnetic flux density due to the single wire as

$$\mathbf{B} = \frac{\mu_0 I_1}{2\pi r}\,\mathbf{a}_\phi$$

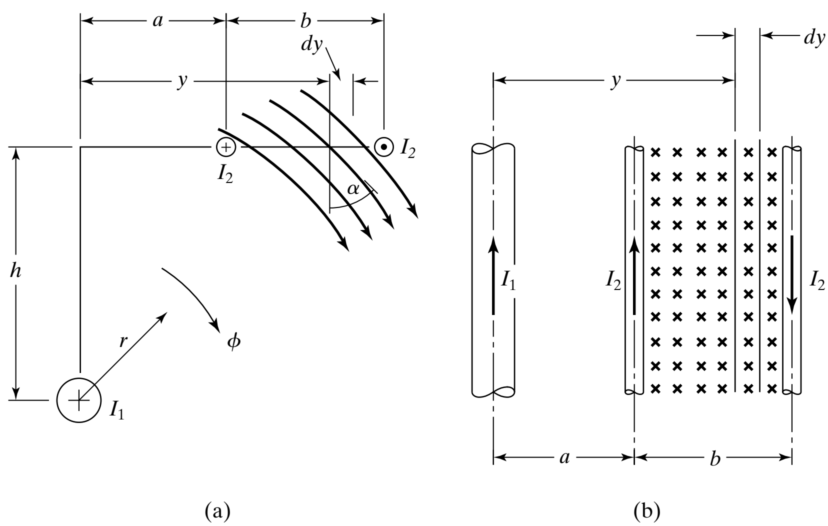

FIGURE 5.17

For the computation of mutual inductance per unit length between a two-wire telephone line and a single wire parallel to it.

The flux $d\psi_{21}$ crossing a rectangular surface of length unity and width dy lying between the telephone wires, as shown in Fig. 5.17(b), is then given by

$$d\psi_{21} = B\,dy\cos\alpha = \frac{\mu_0 I_1 y}{2\pi(h^2 + y^2)}\,dy$$

where α is the angle between the flux lines and the normal to the rectangular surface, as shown in Fig. 5.17(a). The total flux ψ_{21} crossing the rectangular surface of length unity and extending from one telephone wire to the other is

$$\psi_{21} = \int_{y=a}^{a+b} d\psi_{21} = \int_{y=a}^{a+b} \frac{\mu_0 I_1 y}{2\pi(h^2 + y^2)}\,dy$$
$$= \frac{\mu_0 I_1}{4\pi}\ln\frac{h^2 + (a+b)^2}{h^2 + a^2}$$

This is the flux due to I_1 linking I_2 per unit length along the wires. Thus, the required mutual inductance per unit length of the wires is given by

$$\mathcal{L}_{21} = \frac{\psi_{21}}{I_1} = \frac{\mu_0}{4\pi}\ln\frac{h^2 + (a+b)^2}{h^2 + a^2}\ \text{H/m}$$

K5.4. Infinitely long, coaxial cylindrical arrangement; Capacitance per unit length ($\mathscr{C}$); Conductance per unit length ($\mathscr{G}$); Inductance per unit length ($\mathcal{L}$); Relationship between $\mathscr{C}$, $\mathscr{G}$, and $\mathcal{L}$; Parallel cylindrical wire arrangement; Internal inductance; Mutual inductance.

D5.9. A coaxial cylindrical conductor arrangement [see Fig. 5.13(b)] has the dimensions $a = 1$ cm and $b = 3$ cm. **(a)** By what value of the distance d should the inner conductor be displaced parallel to the outer conductor [see Fig. 5.13(d)] to increase the capacitance per unit length of the arrangement by 25%? **(b)** By what percentage is the inductance per unit length of the arrangement then changed from the original value?

Ans. **(a)** 1.2368 cm; **(b)** −20.

D5.10. Figure 5.18 is the cross-sectional view of the coaxial cylindrical conductor arrangement in which a solid conductor of radius a is enclosed by a hollow conductor of inner radius $4a$ and outer radius $5a$. Current I_0 flows in the inner conductor in the $+z$-direction and returns on the outer conductor in the $-z$-direction with densities given by

$$\mathbf{J} = \begin{cases} \dfrac{I_0 e}{\pi a^2}(1 - e^{-r^2/a^2})\mathbf{a}_z & \text{for} \quad 0 < r < a \\ -\dfrac{I_0}{9\pi a^2}\mathbf{a}_z & \text{for} \quad 4a < r < 5a \end{cases}$$

Find the value of N, the fraction of the current I_0 linked by the magnetic flux $d\psi_i$ at a given radius r, for each of the following values of r: **(a)** $0.8a$; **(b)** $3a$; and **(c)** $4.5a$.

Ans. **(a)** 0.4547; **(b)** 1; **(c)** 0.5278.

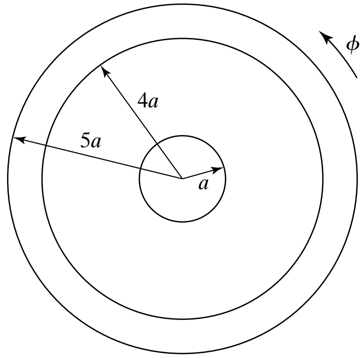

FIGURE 5.18
For Problem D5.9

5.5 ELECTRIC- AND MAGNETIC-FIELD SYSTEMS

In Section 3.1, we discussed briefly how lumped circuit theory is based upon approximations resulting from the neglect of certain terms in one or both of Maxwell's curl equations. Such approximations, valid at low frequencies, are known as *quasistatic approximations*. In this section, we illustrate the determination of the low-frequency terminal behavior of a physical structure via a quasistatic extension of the static field existing in the structure when the frequency of the source driving the structure is zero. The quasistatic extension consists of starting with a time-varying field having the same spatial characteristics as that of the static field, and obtaining the field solutions containing terms up to and including the first power in ω, the radian frequency, leading to the concept of electric- and magnetic-field systems.

Quasistatic field analysis for an inductor

To introduce the quasistatic field approach, we consider the case of an inductor, as represented by the structure shown in Fig. 5.19(a), in which an arrangement of two parallel-plane conductors joined at one end by another conducting sheet is excited by a current source at the other end. We neglect fringing of the fields by assuming that the spacing d between the plates is very small compared with the dimensions of the plates or that the structure is part of a structure of much larger extent in the y- and z-directions. For a constant-current source of value I_0 driving the structure at the end $z = -l$, as shown in the figure, such that the surface current densities on the two plates are given by

$$\mathbf{J}_S = \begin{cases} \dfrac{I_0}{w}\mathbf{a}_z & \text{for} \quad x = 0 \\ -\dfrac{I_0}{w}\mathbf{a}_z & \text{for} \quad x = d \end{cases} \tag{5.83}$$

the medium between the plates is characterized by a uniform y-directed magnetic field, as shown by the cross-sectional view in Fig. 5.19(b). From the boundary condition for the tangential magnetic-field intensity at the surface of a perfect

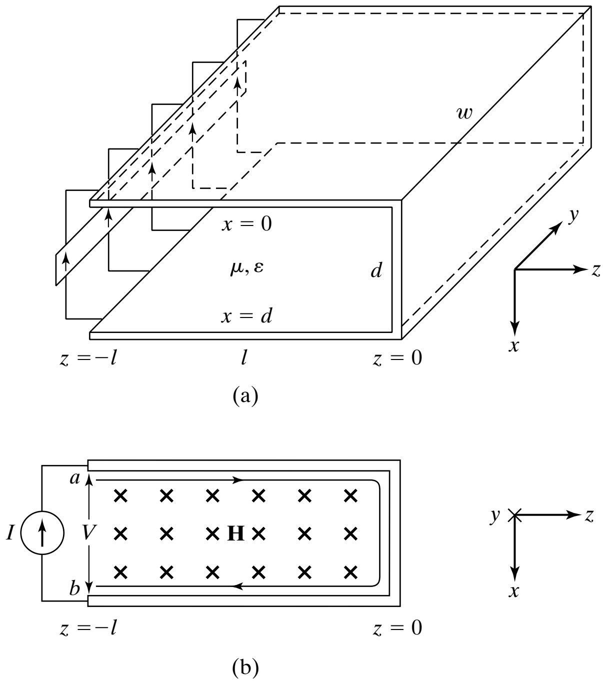

FIGURE 5.19

(a) Parallel-plate structure short-circuited at one end and driven by a current source at the other end. (b) Magnetic field between the plates for a constant-current source.

conductor, the magnitude of this field is I_0/w. Thus, we obtain the static magnetic-field intensity between the plates to be

$$\mathbf{H} = \frac{I_0}{w}\mathbf{a}_y \qquad \text{for} \quad 0 < x < d \tag{5.84}$$

The field is zero outside the plates.

The corresponding magnetic flux density is given by

$$\mathbf{B} = \mu\mathbf{H} = \frac{\mu I_0}{w}\mathbf{a}_y \qquad \text{for} \quad 0 < x < d \tag{5.85}$$

The magnetic flux ψ linking the current is simply the flux crossing the cross-sectional plane of the structure. Since **B** is uniform in the cross-sectional plane and normal to it,

$$\psi = B_y(dl) = \frac{\mu dl}{w} I_0 \tag{5.86}$$

The ratio of this magnetic flux to the current, that is, the inductance of the structure, is given by

$$\boxed{L = \frac{\psi}{I_0} = \frac{\mu dl}{w}} \tag{5.87}$$

To discuss the quasistatic behavior of the structure, we now let the current source vary sinusoidally with time at a frequency ω and assume that the magnetic field between the plates varies accordingly. Thus for

$$I(t) = I_0 \cos \omega t \tag{5.88}$$

we have

$$\mathbf{H}_0 = \frac{I_0}{w} \cos \omega t \, \mathbf{a}_y \tag{5.89}$$

where the subscript 0 denotes that the field is of the zeroth power in ω. In terms of phasor notation, we have

$$\boxed{\begin{aligned} \bar{I} &= I_0 \qquad (5.90) \\ \bar{H}_{y0} &= \frac{I_0}{w} \qquad (5.91) \end{aligned}}$$

The time-varying magnetic field (5.87) gives rise to an electric field in accordance with Maxwell's curl equation for **E**. Expansion of the curl equation for the case under consideration gives

$$\frac{\partial E_x}{\partial z} = -\frac{\partial B_{y0}}{\partial t} = -\mu \frac{\partial H_{y0}}{\partial t}$$

or, in phasor form,

$$\frac{\partial \bar{E}_x}{\partial z} = -j\omega\mu \bar{H}_{y0} \tag{5.92}$$

Substituting for $\bar{H}_{y0}$ from (5.91), we have

$$\frac{\partial \bar{E}_x}{\partial z} = -j\omega\mu \frac{I_0}{w}$$

or

$$\bar{E}_x = -j\omega\mu \frac{I_0}{w} z + \bar{C} \tag{5.93}$$

The constant $\bar{C}$ is, however, equal to zero, since $[\bar{E}_x]_{z=0} = 0$ to satisfy the boundary condition of zero tangential electric field on the perfect conductor surface. Thus, we obtain the quasistatic electric field in the structure to be

$$\boxed{\bar{E}_{x1} = -j\omega \frac{\mu z}{w} I_0} \tag{5.94}$$

where the subscript 1 denotes that the field is of the first power in ω. The value of this field at the input of the structure is given by

$$\boxed{[\bar{E}_{x1}]_{z=-l} = j\omega\mu l \frac{I_0}{w}} \tag{5.95}$$

The voltage developed across the current source is now given by

$$\begin{aligned}\bar{V} &= \int_a^b [\bar{E}_{x1}]_{z=-l}\, dx \\ &= j\omega \frac{\mu d l}{w} I_0\end{aligned}$$

or

$$\boxed{\bar{V} = j\omega L I_0} \tag{5.96}$$

Thus, the quasistatic extension of the static field in the structure of Fig. 5.19 illustrates that its input behavior for low frequencies is essentially that of a single inductor of value equal to that found from static-field considerations.

Validity of quasistatic approximation for an inductor

We shall now determine the condition under which the quasistatic approximation is valid, that is, the condition under which the field of the first power in ω is the predominant part of the total field. To do this, we proceed in the following manner. The electric field $\bar{E}_{x1}$ gives rise to a magnetic field in accordance with Maxwell's curl equation for **H**, which for the case under consideration is given by

$$\frac{\partial H_y}{\partial z} = -\varepsilon \frac{\partial E_x}{\partial t}$$

or in phasor form by

$$\frac{\partial \bar{H}_y}{\partial z} = -j\omega\varepsilon \bar{E}_x \tag{5.97}$$

Substituting $\bar{E}_{x1}$ from (5.94) for $\bar{E}_x$ in (5.97), we have

$$\frac{\partial \bar{H}_y}{\partial z} = -\omega^2 \mu\varepsilon \frac{z}{w} I_0$$

or

$$\bar{H}_{y2} = -\frac{\omega^2 \mu\varepsilon z^2}{2w} I_0 + \bar{C}'' \tag{5.98}$$

where the subscript 2 denotes that the field is of power 2 in ω. The constant $\bar{C}''$ can be evaluated by noting that at $z = -l$, $\bar{H}_{y2}$ must be zero, since $\bar{H}_{y0}$ by itself satisfies the boundary condition $\mathbf{J}_S = \mathbf{a}_n \times \mathbf{H}$. Thus, we get

$$\bar{H}_{y2} = -\frac{\omega^2\mu\varepsilon(z^2 - l^2)}{2w} I_0 \tag{5.99}$$

This magnetic field gives rise to an electric field in accordance with Maxwell's curl equation for $\mathbf{E}$. Hence, we have

$$\begin{aligned}\frac{\partial \bar{E}_x}{\partial z} &= -j\omega\mu\bar{H}_{y2} \\ &= \frac{j\omega^3\mu^2\varepsilon(z^2 - l^2)}{2w} I_0\end{aligned}$$

or

$$\bar{E}_{x3} = \frac{j\omega^3\mu^2\varepsilon(z^3 - 3l^2 z)}{6w} I_0 + \bar{C}''' \tag{5.100}$$

where the subscript 3 denotes that the field is of power 3 in ω. The constant $\bar{C}'''$ has to be equal to zero to satisfy the boundary condition of zero tangential electric field on the conductor surface $z = 0$. Thus, we obtain

$$\bar{E}_{x3} = \frac{j\omega^3\mu^3\varepsilon(z^3 - 3l^2 z)}{6w} I_0 \tag{5.101}$$

and, hence,

$$[\bar{E}_{x3}]_{z=-l} = j\frac{\omega^3\mu^2\varepsilon l^3}{3}\frac{I_0}{w} \tag{5.102}$$

Continuing in this manner, we would obtain

$$[\bar{E}_{x5}]_{z=-l} = j\frac{2\omega^5\mu^3\varepsilon^2 l^5}{15}\frac{I_0}{w} \tag{5.103}$$

and so on. The total electric field at $z = -l$ can then be written as

$$\begin{aligned}[\bar{E}_x]_{z=-l} &= [\bar{E}_{x1}]_{z=-l} + [\bar{E}_{x3}]_{z=-l} + [\bar{E}_{x5}]_{z=-l} + \cdots \\ &= j\omega\mu l\frac{I_0}{w} + j\frac{\omega^3\mu^2\varepsilon l^2}{3}\frac{I_0}{w} + j\frac{2\omega^5\mu^3\varepsilon^2 l^3}{15}\frac{I_0}{w} + \cdots \\ &= j\sqrt{\frac{\mu}{\varepsilon}}\frac{I_0}{w}\left[\omega\sqrt{\mu\varepsilon}l + \frac{1}{3}(\omega\sqrt{\mu\varepsilon}l)^3 + \frac{2}{15}(\omega\sqrt{\mu\varepsilon}l)^5 + \cdots\right]\end{aligned}$$

or

$$\boxed{[\bar{E}_x]_{z=-l} = j\sqrt{\frac{\mu}{\varepsilon}}\frac{I_0}{w}\tan\omega\sqrt{\mu\varepsilon}l} \tag{5.104}$$

From (5.104), it can be seen that for $\omega\sqrt{\mu\varepsilon}l \ll 1$,

$$\begin{aligned}[\bar{E}_x]_{z=-l} &\approx j\sqrt{\frac{\mu}{\varepsilon}}\frac{I_0}{w}\omega\sqrt{\mu\varepsilon}l \\ &= j\omega\mu l\frac{I_0}{w}\end{aligned}$$

which is the same as $[\bar{E}_{x1}]_{z=-l}$. Thus, the condition under which the quasistatic approximation is valid is

$$\omega\sqrt{\mu\varepsilon}l \ll 1$$

or

$$\boxed{f \ll \frac{1}{2\pi\sqrt{\mu\varepsilon}\,l}} \tag{5.105}$$

For frequencies beyond which (5.105) is valid, the input behavior of the structure of Fig. 5.19 is no longer essentially that of a single inductor.

To further investigate the condition for the quasistatic approximation, we recognize that (5.105) can be written as

$$l \ll \frac{v_p}{2\pi f}$$

or,

$$l \ll \frac{\lambda}{2\pi} \tag{5.106}$$

where $\lambda = v_p/f$ is the wavelength corresponding to f in the dielectric region between the plates. Thus, (5.106) tells us that the length of the structure must be very small compared to the wavelength.

Electric- and magnetic-field systems

The criterion (5.106) is a general condition for the quasistatic approximation for the input behavior of a physical structure. Physical structures can be classified as electric-field systems and magnetic-field systems, depending on whether the electric field or the magnetic field is predominant. Quasistatic electric- and magnetic-field systems are particularly important in electromechanics. The structure of Fig. 5.19 is a magnetic-field system, since for the static case the only field present between the plates is the magnetic field and the quasistatic magnetic field has the same spatial dependence as that of the static magnetic field. The quasistatic magnetic field gives rise to a time-varying electric field, but the corresponding displacement current is so small that its effect in adding to the quasistatic magnetic field is negligible, and hence it can be omitted from Maxwell's curl equation for **H**. Thus, for a quasistatic magnetic-field system, we have

$$\nabla \times \mathbf{H} = \mathbf{J} \tag{5.107a}$$

$$\nabla \times \mathbf{E} = -\frac{\partial \mathbf{B}}{\partial t} \tag{5.107b}$$

$$\nabla \cdot \mathbf{B} = 0 \tag{5.107c}$$

Likewise, if the structure of Fig. 5.19 is open-circuited at $z = 0$ and driven by a voltage source at $z = -l$, the only field present between the plates in the static case would be the electric field, and the quasistatic electric field would have the same spatial dependence as that of the static electric field. The system would then be an electric-field system. The quasistatic electric field would give rise to a time-varying magnetic field, but the corresponding value of $\partial \mathbf{B}/\partial t$ would be so small that its effect in adding to the quasistatic electric field would be negligible and, hence, it can be omitted from Maxwell's curl equation for **E**. Thus, for a quasistatic electric-field system, we have

$$\nabla \times \mathbf{E} = \mathbf{0} \tag{5.108a}$$

$$\nabla \times \mathbf{H} = \mathbf{J} + \frac{\partial \mathbf{D}}{\partial t} \tag{5.108b}$$

$$\nabla \cdot \mathbf{D} = \rho \tag{5.108c}$$

When the medium between the plates is conductive, a conduction current flows between the plates in accordance with $\mathbf{J} = \mathbf{J}_c = \sigma\mathbf{E}$ and the analysis for low-frequency input behavior results in both electric and magnetic fields of the first order in ω. We shall illustrate this by means of an example.

Example 5.10 Determination of low-frequency behavior of a resistor by quasistatic field approach

Low-frequency behavior of a resistor

Let us consider the case of two parallel perfectly conducting plates separated by a lossy medium characterized by conductivity σ, permittivity ε, and permeability μ, and driven by a voltage source at one end, as shown in Fig. 5.20(a). We wish to determine its low-frequency behavior by using the quasistatic-field approach.

Assuming the voltage source to be a constant-voltage source, we first obtain the static electric field in the medium between the plates to be

$$\mathbf{E} = \frac{V_0}{d}\mathbf{a}_x$$

following the procedure of Example 5.6. The conduction current density in the medium is then given by

$$\mathbf{J}_c = \sigma\mathbf{E} = \frac{\sigma V_0}{d}\mathbf{a}_x$$

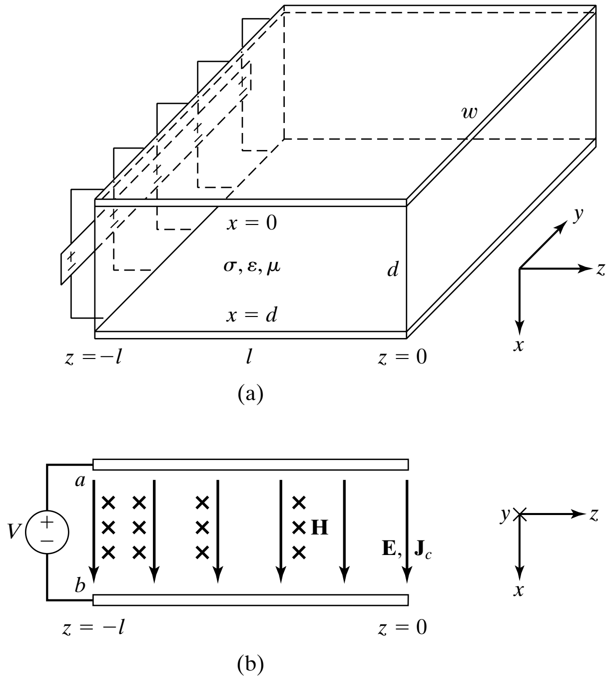

FIGURE 5.20

(a) Parallel-plate structure with lossy medium between the plates and driven by a voltage source. (b) Electric and magnetic fields between the plates for a constant-voltage source.

The conduction current gives rise to a static magnetic field in accordance with Maxwell's curl equation for **H**, given for static fields by

$$\nabla \times \mathbf{H} = \mathbf{J}_c = \sigma \mathbf{E}$$

For the case under consideration, this reduces to

$$\frac{\partial H_y}{\partial z} = -\sigma E_x = -\frac{\sigma V_0}{d}$$

giving us

$$H_y = -\frac{\sigma V_0 z}{d} + C_1$$

The constant C_1 is, however, equal to zero, since $[H_y]_{z=0} = 0$ in view of the boundary condition that the surface current density on the plates must be zero at $z = 0$. Thus, the static magnetic field in the medium between the plates is given by

$$\mathbf{H} = -\frac{\sigma V_0 z}{d}\mathbf{a}_y$$

The static electric- and magnetic-field distributions are shown by the cross-sectional view of the structure in Fig. 5.20(b).

To determine the quasistatic behavior of the structure, we now let the voltage source vary sinusoidally with time at a frequency ω and assume that the electric and magnetic fields vary with time accordingly. Thus, for

$$V = V_0 \cos \omega t$$

we have

$$\mathbf{E}_0 = \frac{V_0}{d} \cos \omega t \, \mathbf{a}_x \tag{5.109a}$$

$$\mathbf{H}_0 = -\frac{\sigma V_0 z}{d} \cos \omega t \, \mathbf{a}_y \tag{5.109b}$$

where the subscript 0 denotes that the fields are of the zeroth power in ω. In terms of phasor notation, we have for $\bar{V} = V_0$,

$$\bar{E}_{x0} = \frac{V_0}{d} \tag{5.110a}$$

$$\bar{H}_{y0} = -\frac{\sigma V_0 z}{d} \tag{5.110b}$$

The time-varying electric field (5.109a) gives rise to a magnetic field in accordance with

$$\nabla \times \mathbf{H} = \frac{\partial \mathbf{D}_0}{\partial t} = \varepsilon \frac{\partial \mathbf{E}_0}{\partial t}$$

and the time-varying magnetic field (5.109b) gives rise to an electric field in accordance with

$$\nabla \times \mathbf{E} = \frac{\partial \mathbf{B}_0}{\partial t} = -\mu \frac{\partial \mathbf{H}_0}{\partial t}$$

For the case under consideration and using phasor notation, these equations reduce to

$$\frac{\partial \bar{H}_y}{\partial z} = -j\omega\varepsilon \bar{E}_{x0} = -j\omega \frac{\varepsilon V_0}{d}$$

$$\frac{\partial \bar{E}_x}{\partial z} = -j\omega\mu \bar{H}_{y0} = j\omega \frac{\mu\sigma V_0 z}{d}$$

giving us

$$\bar{H}_{y1} = -j\omega \frac{\varepsilon V_0 z}{d} + \bar{C}_2$$

$$\bar{E}_{x1} = j\omega \frac{\mu\sigma V_0 z^2}{2d} + \bar{C}_3$$

where the subscript 1 denotes that the fields are of the first power in ω. The constant $\bar{C}_2$ is, however, equal to zero in view of the boundary condition that the surface current density on the plates must be zero at $z = 0$. To evaluate the constant $\bar{C}_3$, we note that $[\bar{E}_{x1}]_{z=-l} = 0$, since the boundary condition at the source end, that is,

$$\bar{V} = \int_a^b [\bar{E}_x]_{z=-l} \, dx$$

is satisfied by $\bar{E}_{x0}$ alone. Thus, we have

$$j\omega\frac{\mu\sigma V_0(-l)^2}{2d} + \overline{C}_3 = 0$$

or

$$\overline{C}_3 = -j\omega\frac{\mu\sigma V_0 l^2}{2d}$$

Substituting for $\overline{C}_3$ and $\overline{C}_2$ in the expressions for $\bar{E}_{x1}$ and $\bar{H}_{y1}$, respectively, we get

$$\bar{E}_{x1} = j\omega\frac{\mu\sigma V_0(z^2 - l^2)}{2d} \tag{5.111a}$$

$$\bar{H}_{y1} = -j\omega\frac{\varepsilon V_0 z}{d}$$

The result for $\bar{H}_{y1}$ is, however, not complete, since $\bar{E}_{x1}$ gives rise to a conduction current of density proportional to ω, which in turn provides an additional contribution to $\bar{H}_{y1}$. Denoting this contribution to be $\bar{H}^c_{y1}$, we have

$$\frac{\partial \bar{H}^c_{y1}}{\partial z} = -\sigma\bar{E}_{x1} = -j\omega\frac{\mu\sigma^2 V_0(z^2 - l^2)}{2d}$$

$$\bar{H}^c_{y1} = -j\omega\frac{\mu\sigma^2 V_0(z^3 - 3zl^2)}{6d} + \overline{C}_4$$

The constant $\overline{C}_4$ is zero for the same reason that $\overline{C}_2$ is zero. Hence, setting $\overline{C}_4$ equal to zero and adding the resulting expression for $\bar{H}^c_{y1}$ to the right side of the expression for $\bar{H}_{y1}$, we obtain the complete expression for $\bar{H}_{y1}$ as

$$\bar{H}_{y1} = -j\omega\frac{\varepsilon V_0 z}{d} - j\omega\frac{\mu\sigma^2 V_0(z^3 - 3zl^2)}{6d} \tag{5.111b}$$

The total field components correct to the first power in ω are then given by

$$\begin{aligned}\bar{E}_x &= \bar{E}_{x0} + \bar{E}_{x1}\\ &= \frac{V_0}{d} + j\omega\frac{\mu\sigma V_0(z^2 - l^2)}{2d}\end{aligned} \tag{5.112a}$$

$$\begin{aligned}\bar{H}_y &= \bar{H}_{y0} + \bar{H}_{y1}\\ &= -\frac{\sigma V_0 z}{d} - j\omega\frac{\varepsilon V_0 z}{d} - j\omega\frac{\mu\sigma^2 V_0(z^3 - 3zl^2)}{6d}\end{aligned} \tag{5.112b}$$

The current drawn from the voltage source is

$$\begin{aligned}\bar{I} &= w[\bar{H}_y]_{z=-l}\\ &= \left(\frac{\sigma w l}{d} + j\omega\frac{\varepsilon w l}{d} - j\omega\frac{\mu\sigma^2 w l^3}{3d}\right)\overline{V}\end{aligned} \tag{5.113}$$

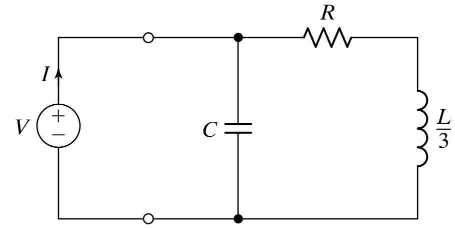

FIGURE 5.21

Equivalent circuit for the low-frequency input behavior of the structure of Fig. 5.20.

Finally, the input admittance of the structure is given by

$$\begin{aligned}\bar{Y} &= \frac{\bar{I}}{\bar{V}} = j\omega\frac{\varepsilon wl}{d} + \frac{\sigma wl}{d}\left(1 - j\omega\frac{\mu\sigma l^2}{3}\right)\\ &\approx j\omega\frac{\varepsilon wl}{d} + \frac{1}{\dfrac{d}{\sigma wl}\left(1 + j\omega\dfrac{\mu\sigma l^2}{3}\right)}\end{aligned} \tag{5.114}$$

where we have approximated $[1 - j\omega(\mu\sigma l^2/3)]$ by $[1 + j\omega(\mu\sigma l^2/3)]^{-1}$. Proceeding further, we have

$$\begin{aligned}\bar{Y} &= j\omega\frac{\varepsilon wl}{d} + \frac{1}{\dfrac{d}{\sigma wl} + j\omega\dfrac{\mu dl}{3w}}\\ &= j\omega C + \frac{1}{R + (j\omega L/3)}\end{aligned} \tag{5.115}$$

where $C = \varepsilon wl/d$ is the capacitance of the structure if the material is a perfect dielectric, $R = d/\sigma wl$ is the dc resistance (reciprocal of the conductance) of the structure, and $L = \mu dl/w$ is the inductance of the structure if the material is lossless and the two plates are short-circuited at $z = 0$. The equivalent circuit corresponding to (5.115) consists of capacitance C in parallel with the series combination of resistance R and inductance $L/3$, as shown in Fig. 5.21. Thus, the low-frequency input behavior of the structure of Fig. 5.20 (which acts like a pure resistor at dc) can be represented by the circuit Fig. 5.21, with the understanding of the approximation used in (5.114).

Note that for $\sigma = 0$, (5.113) reduces to

$$\begin{aligned}\bar{I} &= j\omega\frac{\varepsilon wl}{d}\bar{V}\\ &= j\omega C\bar{V}\end{aligned}$$

and the input behavior of the structure is essentially that of a single capacitor of the same value as that found from static-field considerations.

Beyond quasistatics

Sometimes, it is of interest to consider equivalent circuit representation for the input behavior of a structure for frequencies beyond the quasistatic approximation. For an example, let us consider frequencies slightly beyond those for which the quasistatic approximation is valid for the structure of Fig. 5.19. Then

$$[\bar{E}_x]_{z=-l} = [\bar{E}_{x1}]_{z=-l} + [\bar{E}_{x3}]_{z=-l}$$

and from (5.95) and (5.102), we have

$$[\bar{E}_x]_{z=-l} \approx j\omega\mu l \frac{\bar{I}_0}{w} + j\frac{\omega^3\mu^2\varepsilon l^2}{3}\frac{\bar{I}_0}{w} \tag{5.116}$$

and the voltage developed across the current source is given by

$$\begin{aligned}
\bar{V} &= \int_a^b [\bar{E}_x]_{z=-l}\,dx \\
&\approx j\omega\frac{\mu dl}{w}\bar{I}_0 + j\frac{\omega^3\mu^2\varepsilon dl^2}{3}\frac{\bar{I}_0}{w} \\
&= j\omega\frac{\mu dl}{w}\bar{I}_0\left[1 + \frac{1}{3}\omega^2\left(\frac{\mu dl}{w}\right)\left(\frac{\varepsilon wl}{d}\right)\right] \\
&= j\omega L\bar{I}_0\left[1 + \frac{1}{3}\omega^2 LC\right]
\end{aligned} \tag{5.117}$$

where $C = \varepsilon wl/d$ is the capacitance of the structure with the end $z = 0$ open-circuited and from static-field considerations. Rearranging (5.117), we get

$$\begin{aligned}
\bar{I}_0 &= \frac{\bar{V}}{j\omega L\left(1 + \frac{1}{3}\omega^2 LC\right)} \\
&\approx \frac{\bar{V}}{j\omega L}\left(1 - \frac{1}{3}\omega^2 LC\right) \\
&= \bar{V}\left(\frac{1}{j\omega L} + j\omega\frac{C}{3}\right)
\end{aligned} \tag{5.118}$$

Thus, the equivalent circuit consists of the parallel combination of L and $\frac{1}{3}C$, as shown in Fig. 5.22.

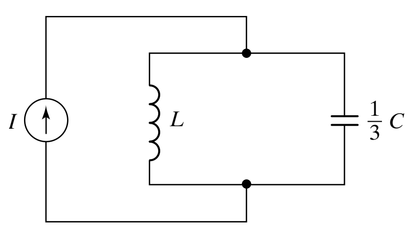

FIGURE 5.22

Equivalent circuit for the input behavior of the structure of Fig. 5.19 for frequencies slightly beyond those for which the quasistatic approximation is valid.

K5.5. Quasistatic approximation; Condition for quasistatic approximation; Electric- and magnetic-field systems; Low-frequency terminal behavior; Inductor; Resistor.

D5.11. For the structure of Fig. 5.19, assume that $l = 10$ cm, $d = 1$ cm, $w = 10$ cm, and that the medium between the conductors is free space. Assuming that the condition for quasistatic approximation given by (5.105) is valid for $f < 1/20\pi\sqrt{\mu\varepsilon}l$, find the following: **(a)** the maximum frequency for which the input behavior of the structure is essentially that of a single inductor; **(b)** the value of this inductor; and **(c)** the ratio of the amplitude of the electric field at the input, if the structure behaves exactly like a single inductor, to the amplitude of the actual electric field at the input for the frequency found in (a).

Ans. **(a)** 47.746 MHz; **(b)** $4\pi \times 10^{-9}$ H; **(c)** 0.9967.

5.6 MAGNETIC CIRCUITS

Toroidal conductor versus toroidal magnetic core

Let us consider the two structures shown in Fig. 5.23. The structure of Fig. 5.23(a) is a toroidal conductor of uniform conductivity σ and has a cross-sectional area A and mean circumference l. There is an infinitesimal gap a–b across which a potential difference of V_0 volts is maintained by connecting an appropriate voltage source. Because of the potential difference, an electric field is established in the toroid and a conduction current I_c results from the higher-potential surface a to the lower-potential surface b as shown in the figure. The structure of Fig. 5.23(b) is a toroidal magnetic core of uniform permeability μ with a cross-sectional area A and mean circumference l. A current I A is passed through a filamentary wire of N turns wound around the toroid by connecting an appropriate current source. Because of the current through the winding, a magnetic field is established in the toroid and a magnetic flux ψ results in the direction of advance of a right-hand screw as it is turned in the sense of the current.

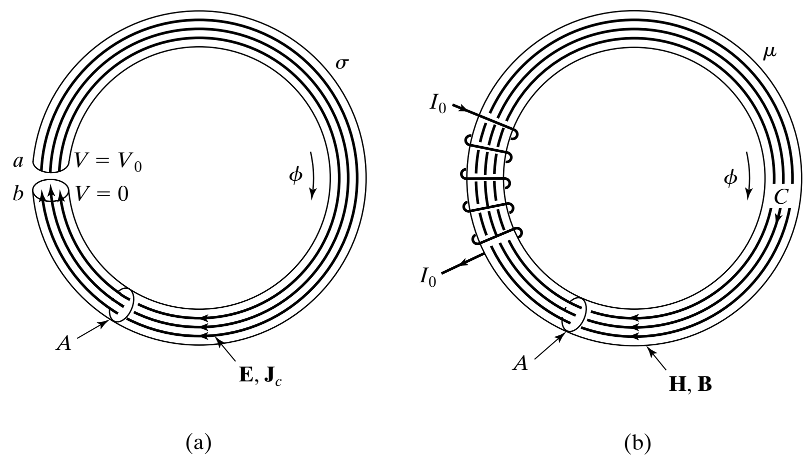

FIGURE 5.23

(a) Toroidal conductor. (b) Toroidal magnetic core.

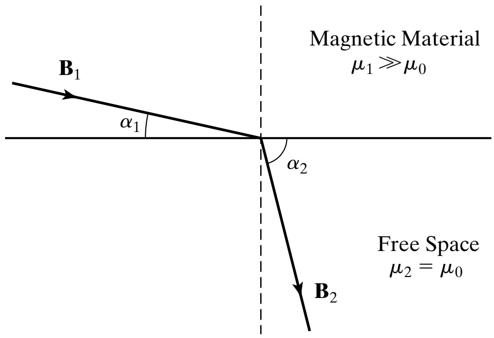

FIGURE 5.24

Lines of magnetic flux density at the boundary between free space and a magnetic material of $\mu \gg \mu_0$.

Since the conduction current cannot leak into the free space surrounding the conductor, it is confined entirely to the conductor. On the other hand, the magnetic flux can leak into the free space surrounding the magnetic core and, hence, is not confined completely to the core. However, let us consider the case for which $\mu \gg \mu_0$. Applying the boundary conditions at the boundary between a magnetic material of $\mu \gg \mu_0$ and free space, as shown in Fig. 5.24, we have

$$B_1 \sin \alpha_1 = B_2 \sin \alpha_2$$
$$H_1 \cos \alpha_1 = H_2 \cos \alpha_2$$

or

$$\frac{B_1}{H_1} \tan \alpha_1 = \frac{B_2}{H_2} \tan \alpha_2$$
$$\frac{\tan \alpha_1}{\tan \alpha_2} = \frac{\mu_2}{\mu_1} \ll 1$$

Thus, $\alpha_1 \ll \alpha_2$, and

$$\frac{B_2}{B_1} = \frac{\sin \alpha_1}{\sin \alpha_2} \ll 1$$

For example, if the values of μ_1 and α_2 are $1000\mu_0$ and $89°$, respectively, then $\alpha_1 = 3°16'$ and $\sin \alpha_1 / \sin \alpha_2 = 0.057$. We can assume, for all practical purposes, that the magnetic flux is confined to the magnetic core, just as the conduction current is confined to the conductor. The structure of Fig. 5.23(b) is then known as a *magnetic circuit*, similar to the *electric circuit* of Fig. 5.23(a). Magnetic circuits are encountered in applications involving electromechanical systems, typical examples of which are electromagnets, transformers, and rotating machines.

For the toroidal conductor of Fig. 5.23(a), we have

$$\int_a^b \mathbf{E} \cdot d\mathbf{l} = V_0 \tag{5.119}$$

Proceeding with the assumption that E_ϕ is uniform over the cross-sectional area and equal to its value E_m at the mean radius of the toroid, and we obtain

$$\begin{aligned} lE_m &= V_0 \\ E_m &= \frac{V_0}{l} \\ J_c &= \sigma E_m = \frac{\sigma V_0}{l} \\ I_c &= J_c A = \frac{\sigma V_0 A}{l} \end{aligned}$$

Thus, the resistance of the circuit is given by

$$R = \frac{V_0}{I_0} = \frac{l}{\sigma A} \tag{5.120}$$

Similarly, for the toroidal magnetic core of Fig. 5.23(b),

$$\oint_C \mathbf{H} \cdot d\mathbf{l} = NI_0 \tag{5.121}$$

Assuming H_ϕ to be uniform over the cross-sectional area and equal to its value H_m at the mean radius of the toroid, we obtain

$$\begin{aligned} lH_m &= NI_0 \\ H_m &= \frac{NI_0}{l} \\ B_m &= \mu H_m = \frac{\mu NI_0}{l} \\ \psi &= B_m A = \frac{\mu NI_0 A}{l} \end{aligned}$$

Reluctance defined

We now define the *reluctance* of the magnetic circuit, denoted by the symbol $\mathcal{R}$, as the ratio of the ampere turns NI_0 applied to the magnetic circuit to the magnetic flux ψ. Thus,

$$\boxed{\mathcal{R} = \frac{NI_0}{\psi} = \frac{l}{\mu A}} \tag{5.122}$$

The reluctance of the magnetic circuit is analogous to the resistance of an electric circuit and has the units of ampere-turns per weber (A-t/Wb). In fact, the complete analogy between the toroidal conductor and the toroidal magnetic core can be seen as follows.

$$V_0 \leftrightarrow NI_0$$
$$\mathbf{E} \leftrightarrow \mathbf{H}$$
$$\mathbf{J}_c \leftrightarrow \mathbf{B}$$
$$\sigma \leftrightarrow \mu$$
$$I_c \leftrightarrow \psi$$
$$R \leftrightarrow \mathcal{R}$$

The equivalent-circuit representations of the two arrangements are shown in Figs. 5.25(a) and (b), respectively. We note from (5.122) that for a given magnetic material, the reluctance appears to be purely a function of the dimensions of the circuit. This is, however, not true, since, for the ferromagnetic materials used for the cores, μ is a function of the magnetic flux density in the material, as we learned in Section 4.3.

As a numerical example of computations involving the magnetic circuit of Fig. 5.23(b), let us consider a core of cross-sectional area 2 cm^2 and mean circumference 20 cm. Let the material of the core be annealed sheet steel for which the B versus H relationship is shown by the curve of Fig. 5.26. Then to establish a magnetic flux of 3×10^{-4} Wb in the core, the mean flux density must

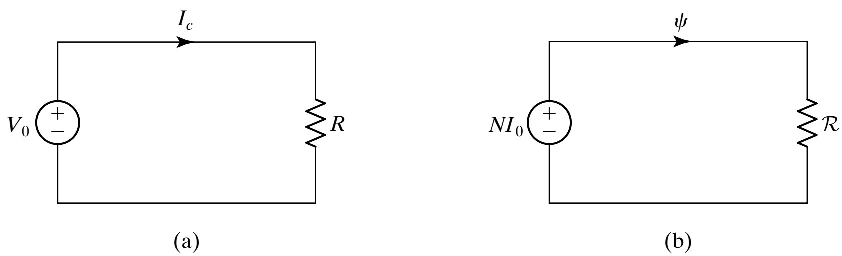

FIGURE 5.25

Equivalent-circuit representations for the structures of Figs. 5.23(a) and (b), respectively.

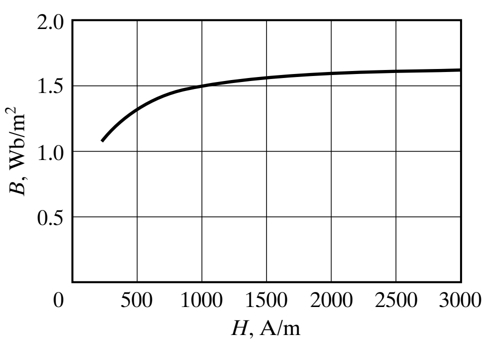

FIGURE 5.26

B versus H curve for annealed sheet steel.

be $(3 \times 10^{-4})/(2 \times 10^{-4})$, or 1.5 Wb/m^2. From Fig. 5.26, the corresponding value of H is 1000 A/m. The number of ampere-turns required to establish the flux is then equal to $1000 \times 20 \times 10^{-2}$, or 200, and the reluctance of the core is $200/(3 \times 10^{-4})$, or $(2/3) \times 10^6$ A-t/Wb. We shall now consider a more detailed example.

Example 5.11 Determination of the ampere-turns for a specified flux in the air gap of a magnetic circuit

Magnetic circuit with three legs and an air gap

A magnetic circuit containing three legs and with an air gap in the right leg is shown in Fig. 5.27(a). A filamentary wire of N turns carrying current I is wound around the center leg. The core material is annealed sheet steel, for which the B versus H relationship is shown in Fig. 5.26. The dimensions of the magnetic circuit are

$$A_1 = A_3 = 3 \text{ cm}^2 \qquad A_2 = 6 \text{ cm}^2$$
$$l_1 = l_3 = 20 \text{ cm} \qquad l_2 = 10 \text{ cm} \qquad l_g = 0.2 \text{ mm}$$

Let us determine the value of NI required to establish a magnetic flux of 4×10^{-4} Wb in the air gap.

The current in the winding establishes a magnetic flux in the center leg that divides between the right and left legs. Fringing of the flux occurs in the air gap, as shown in Fig. 5.27(b). This is taken into account by using an effective cross section larger than the actual cross section, as shown in Fig. 5.27(c). Using subscripts 1, 2, 3, and g for the quantities associated with the left, center, and right legs, and the air gap, respectively, we can write

$$\psi_3 = \psi_g$$
$$\psi_2 = \psi_1 + \psi_3$$

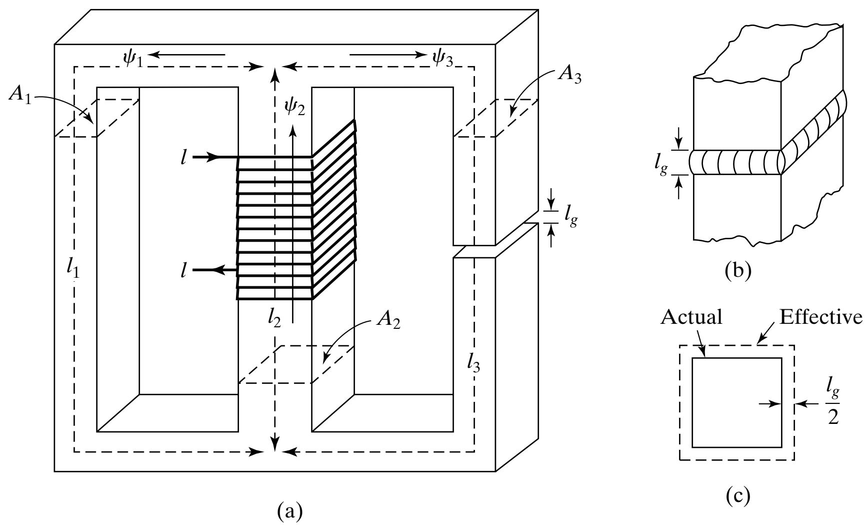

FIGURE 5.27

(a) Magnetic circuit. (b) Fringing of magnetic flux in the air gap of the magnetic circuit. (c) Effective and actual cross sections for the air gap.

Also, applying Ampère's circuital law to the right and left loops of the magnetic circuit, we obtain, respectively,

$$NI = H_2 l_2 + H_3 l_3 + H_g l_g$$
$$NI = H_2 l_2 + H_1 l_1$$

It follows from these two equations that

$$H_1 l_1 = H_3 l_3 + H_g l_g$$

which can also be written directly from a consideration of the outer loop of the magnetic circuit.

Noting from Fig. 5.27(c) that the effective cross section of the air gap is $(\sqrt{3} + l_g)^2 = 3.07 \text{ cm}^2$, we find the required magnetic flux density in the air gap to be

$$B_g = \frac{\psi_g}{(A_g)_{\text{eff}}} = \frac{4 \times 10^{-4}}{3.07 \times 10^{-4}} = 1.303 \text{ Wb/m}^2$$

The magnetic-field intensity in the air gap is

$$H_g = \frac{B_g}{\mu_0} = \frac{1.303}{4\pi \times 10^{-7}} = 0.1037 \times 10^7 \text{ A/m}$$

The flux density in leg 3 is

$$B_3 = \frac{\psi_3}{A_3} = \frac{\psi_g}{A_3} = \frac{4 \times 10^{-4}}{3 \times 10^{-4}} = 1.333 \text{ Wb/m}^2$$

From Fig. 5.26, the value of H_3 is 475 A/m.

Knowing the values of H_g and H_3, we then obtain

$$\begin{aligned} H_1 l_1 &= H_3 l_3 + H_g l_g \\ &= 475 \times 0.2 + 0.1037 \times 10^7 \times 0.2 \times 10^{-3} \\ &= 302.4 \text{ A} \\ H_1 &= \frac{302.4}{0.2} = 1512 \text{ A/m} \end{aligned}$$

From Fig. 5.26, the value of B_1 is 1.56 Wb/m^2, and, hence, the flux in leg 1 is

$$\psi_1 = B_1 A_1 = 1.56 \times 3 \times 10^{-4} = 4.68 \times 10^{-4} \text{ Wb}$$

Thus,

$$\begin{aligned} \psi_2 &= \psi_1 + \psi_3 \\ &= 4.68 \times 10^{-4} + 4 \times 10^{-4} = 8.68 \times 10^{-4} \text{ Wb} \\ B_2 &= \frac{\psi_2}{A_2} = \frac{8.68 \times 10^{-4}}{6 \times 10^{-4}} = 1.447 \text{ Wb/m}^2 \end{aligned}$$

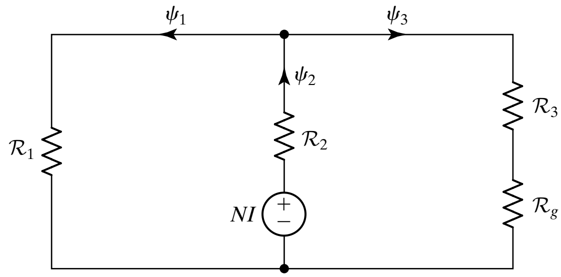

FIGURE 5.28

Equivalent circuit for the magnetic circuit of Fig. 5.27.

From Fig. 5.26, the value of H_2 is 750 A/m. Finally, we obtain the required number of ampere-turns to be

$$\begin{aligned} NI &= H_2 l_2 + H_1 l_1 \\ &= 750 \times 0.1 + 302.4 \\ &= 377.4 \end{aligned}$$

Note that the equivalent circuit corresponding to the magnetic circuit is as shown in Fig. 5.28, where the reluctances are given by

$$\begin{aligned} \mathcal{R}_1 &= \frac{l_1}{\mu_1 A_1} = \frac{H_1 l_1}{B_1 A_1} = \frac{1512 \times 0.2}{1.56 \times 3 \times 10^{-4}} = 646{,}154 \text{ A-t/Wb} \\ \mathcal{R}_2 &= \frac{l_2}{\mu_2 A_2} = \frac{H_2 l_2}{B_2 A_2} = \frac{750 \times 0.1}{1.447 \times 6 \times 10^{-4}} = 86{,}386 \text{ A-t/Wb} \\ \mathcal{R}_3 &= \frac{l_3}{\mu_3 A_3} = \frac{H_3 l_3}{B_3 A_3} = \frac{475 \times 0.2}{1.333 \times 3 \times 10^{-4}} = 237{,}559 \text{ A-t/Wb} \\ \mathcal{R}_g &= \frac{l_g}{\mu_0 (A_g)_{\text{eff}}} = \frac{0.2 \times 10^{-3}}{4\pi \times 10^{-7} \times 3.07 \times 10^{-4}} = 518{,}420 \text{ A-t/Wb} \end{aligned}$$

K5.6. Magnetic circuit; Analogy with electric circuit; Reluctance; Air gap.

D5.12. Assume that the portion of B versus H curve of Fig. 5.26 in the range $1500 \leq H \leq 3000$ can be approximated by the straight line

$$B = 1.5 + 5 \times 10^{-5} H$$

For a toroidal magnetic circuit made of annealed sheet steel, find the reluctance for each of the following cases: **(a)** $A = 4\ \text{cm}^2, l = 30\ \text{cm}, H = 1800$ A/m; **(b)** $A = 2\ \text{cm}^2, l = 20\ \text{cm}, NI = 500$ A-t; and **(c)** $A = 5\ \text{cm}^2, l = 25\ \text{cm}, \psi = 8 \times 10^{-4}$ Wb.

Ans. **(a)** 849,057 A-t/Wb; **(b)** 1,538,462 A-t/Wb; **(c)** 625,000 A-t/Wb.

D5.13. For the magnetic circuit of Fig. 5.27, assume that the region of operation on the B–H curve of the material is such that μ_r of the material is equal to 4000 for all three legs. Find the reluctance as viewed by the excitation for each of the following cases: **(a)** winding in leg 1; **(b)** winding in leg 2; and **(c)** winding in leg 3.

Ans. **(a)** 164,207 A-t/Wb; **(b)** 143,681 A-t/Wb; **(c)** 689,671 A-t/Wb.

5.7 ELECTROMECHANICAL ENERGY CONVERSION

Parallel-plate capacitor with a movable plate

Let us consider a parallel-plate capacitor with one plate fixed and the other plate free to move, as shown by a cross-sectional view in Fig. 5.29. If we assume a positive charge Q on the movable plate and a negative charge $-Q$ on the fixed plate, resulting from the application of a voltage V between the plates, then a force $\mathbf{F}_e$ directed toward the fixed plate is exerted on the movable plate. If this force is allowed to produce a displacement of the movable plate, mechanical work results, thereby converting electrical energy in the system into mechanical energy. Conversely, an externally applied mechanical force can be made to act on the movable plate so as to increase the stored electrical energy in the system. Thus, energy can be converted from electrical to mechanical or vice versa. A familiar example of the former is in the case of an electrical motor, whereas that of the latter is in the case of an electrical generator. To determine the amount of energy converted from one form to another, we first need to know how to compute the force $\mathbf{F}_e$. In this section, we illustrate this computation and discuss the determination of energy converted from one form to another.

Computation of mechanical force of electric origin

The computation of the mechanical force $\mathbf{F}_e$ of electric origin follows from considerations of energy balance associated with the electromechanical system. The energy balance can be expressed as

$$\boxed{\begin{matrix}\text{Mechanical}\\ \text{energy}\\ \text{input}\end{matrix}} + \boxed{\begin{matrix}\text{Electrical}\\ \text{energy}\\ \text{input}\end{matrix}} = \boxed{\begin{matrix}\text{Increase}\\ \text{in stored}\\ \text{mechanical}\\ \text{energy}\end{matrix}} + \boxed{\begin{matrix}\text{Increase}\\ \text{in stored}\\ \text{electrical}\\ \text{energy}\end{matrix}} + \boxed{\begin{matrix}\text{Energy}\\ \text{dissipated}\end{matrix}} \qquad (5.123)$$

For simplicity, we shall consider the system to be lossless so that the last term on the right side of (5.123) is zero. In using (5.123) to find $\mathbf{F}_e$, we shall apply to the movable element of the system an external force equal to $-\mathbf{F}_e$ and displace the element by an infinitesimal distance in the direction of the external force, so that no change in stored mechanical energy occurs. This eliminates the first term on the right side of (5.123). Thus, with reference to the system of Fig. 5.29, we have

$$-F_{ex}\,dx + VI\,dt = dW_e \qquad (5.124)$$

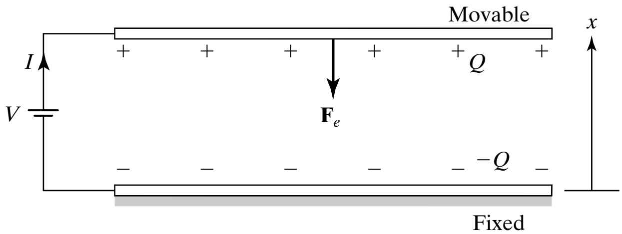

FIGURE 5.29

Parallel-plate capacitor with a movable plate, depicting the force F_e on the movable plate.

where dx is the displacement of the movable plate, I is the current drawn from the voltage source, and W_e is the electric stored energy in the capacitor. Substituting $I = dQ/dt$ from the law of conservation of charge, we obtain

$$-F_{ex}\,dx + V\,dQ = dW_e$$

or

$$\boxed{F_{ex} = -\frac{dW_e}{dx} + V\frac{dQ}{dx}} \tag{5.125}$$

To proceed further, we shall neglect fringing of the electric field at the edges of the capacitor plates so that the charges on the plates and the electric field between the plates are uniformly distributed. Then if A is the area of each plate, we can write the following:

$$\begin{aligned}
W_e &= \frac{1}{2}\varepsilon_0 E^2 Ax = \frac{1}{2}\varepsilon_0\left(\frac{V}{x}\right)^2 Ax \\
&= \frac{\varepsilon_0 V^2 A}{2x} \\
\frac{dW_e}{dx} &= -\frac{\varepsilon_0 V^2 A}{2x^2} \\
Q &= CV = \frac{\varepsilon_0 AV}{x} \\
\frac{dQ}{dx} &= -\frac{\varepsilon_0 AV}{x^2}
\end{aligned}$$

Thus, we obtain

$$\begin{aligned}
F_{ex} &= \frac{\varepsilon_0 V^2 A}{2x^2} - \frac{\varepsilon_0 AV^2}{x^2} \\
&= -\frac{1}{2}\frac{\varepsilon_0 AV^2}{x^2}
\end{aligned} \tag{5.126}$$

Note that in this procedure V was held constant, since the voltage source was kept connected to the capacitor plates in the process of displacing the plate. If, on the other hand, the voltage source is not connected to the capacitor plates in the process of displacing the plate, then Q remains constant, and we can write the following:

$$\begin{aligned}
\frac{dQ}{dx} &= 0 \\
\frac{dW_e}{dx} &= \frac{d}{dx}\left(\frac{1}{2}\varepsilon_0 E^2 Ax\right)
\end{aligned}$$

$$= \frac{d}{dx}\left[\frac{1}{2}\varepsilon_0\left(\frac{Q}{A\varepsilon_0}\right)^2 Ax\right]$$

$$= \frac{1}{2}\frac{Q^2}{A\varepsilon_0}$$

$$F_{ex} = -\frac{1}{2}\frac{Q^2}{A\varepsilon_0} \tag{5.127}$$

The results obtained for F_{ex} in (5.126) and (5.127) appear to be different, but they are not. This can be seen by expressing (5.126) in terms of Q or by expressing (5.127) in terms of V. Choosing the first option, we can write (5.126) as

$$\begin{aligned} F_{ex} &= -\frac{1}{2}\frac{\varepsilon_0 AV^2}{x^2} \\ &= -\frac{1}{2}\varepsilon_0 AE^2 \\ &= -\frac{1}{2}\varepsilon_0 A\left(\frac{Q}{A\varepsilon_0}\right)^2 \\ &= -\frac{1}{2}\frac{Q^2}{A\varepsilon_0} \end{aligned}$$

which is the same as that given by (5.127). This is to be expected since Q and V are not independent of each other; they are related through the capacitance of the capacitor. Thus, the force $\mathbf{F}_e$ is given by

$$\boxed{\mathbf{F}_e = -\frac{1}{2}\frac{\varepsilon_0 AV^2}{x^2}\mathbf{a}_x = -\frac{1}{2}\frac{Q^2}{A\varepsilon_0}\mathbf{a}_x} \tag{5.128}$$

We shall now illustrate, by means of an example, the application of the result we obtained for $\mathbf{F}_e$ in the computation of energy converted from electrical to mechanical, or vice versa, in the energy conversion process.

Example 5.12 Energy conversion in a parallel-plate capacitor with a movable plate

Energy conversion computation

Assume that in the parallel-plate capacitor of Fig. 5.29, a source of mechanical force $\mathbf{F}$ is applied to the movable plate such that $\mathbf{F}$ is always maintained equal to $-\mathbf{F}_e$. By appropriately varying V and $\mathbf{F}$, the system is made to traverse the closed cycle in the Q–x-plane, shown in Fig. 5.30. We wish to calculate the energy converted per cycle and determine whether the conversion is from electrical to mechanical or vice versa.

Since the system is made to traverse a closed cycle in the Q–x-plane, there is no change in the electrical stored energy from the initial state to the final state. Hence, the sum of the mechanical and electrical energy inputs to the system must be zero, or the electrical energy output is equal to the mechanical energy input. The mechanical energy

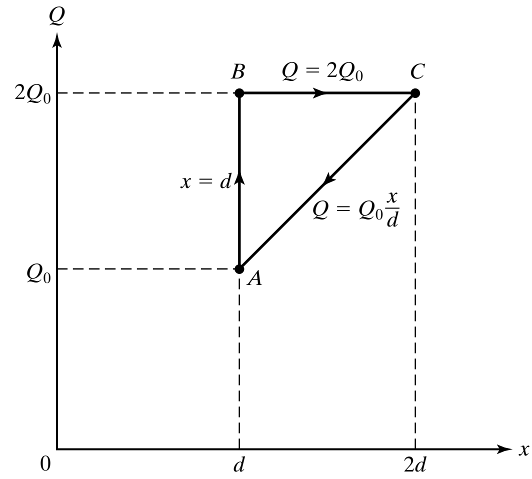

FIGURE 5.30

Closed cycle traversed by the capacitor system of Fig. 5.29.

input is given by

$$\begin{aligned} W_{\text{mechanical input}} &= \oint_{ABCA} F_x\,dx = -\oint_{ABCA} F_{ex}\,dx \\ &= -\int_A^B F_{ex}\,dx - \int_B^C F_{ex}\,dx - \int_C^A F_{ex}\,dx \end{aligned}$$

From A to B, x remains constant; hence, $\int_A^B F_{ex}\,dx$ is zero. From (5.127),

$$F_{ex} = \begin{cases} -\dfrac{2Q_0^2}{A\varepsilon_0} & \text{from} \quad B \text{ to } C \\ -\dfrac{Q_0^2 x^2}{2A\varepsilon_0 d^2} & \text{from} \quad C \text{ to } A \end{cases}$$

Hence,

$$\begin{aligned} W_{\text{mechanical input}} &= \int_{x=d}^{2d} \frac{2Q_0^2}{A\varepsilon_0}\,dx + \int_{x=2d}^{d} \frac{Q_0^2 x^2}{2A\varepsilon_0 d^2}\,dx \\ &= \frac{2Q_0^2 d}{\varepsilon_0 A} - \frac{7Q_0^2 d}{6\varepsilon_0 A} \\ &= \frac{5}{6}\frac{Q_0^2 d}{\varepsilon_0 A} \end{aligned}$$

Thus, an amount of energy equal to $5Q_0^2 d/6\varepsilon_0 A$ is converted from mechanical to electrical form.

Electromagnet

We have thus far considered an electric-field electromechanical system, that is, one in which conversion takes place between energy stored in an electric field and mechanical energy. For an example of a magnetic-field electromechanical

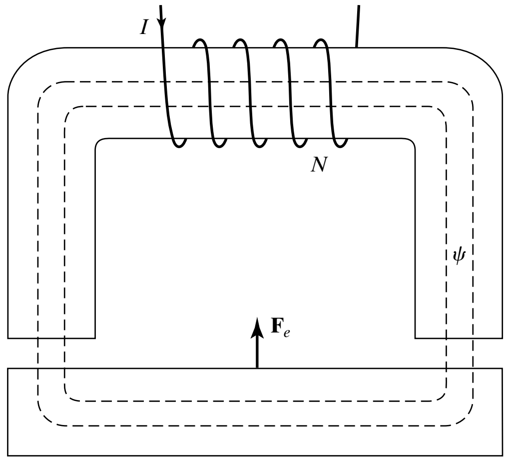

FIGURE 5.31
Electromagnet.

system, that is, one in which conversion takes place between energy stored in a magnetic field and mechanical energy, let us consider the arrangement shown in Fig. 5.31, which is the cross section of an electromagnet. When current is passed through the coil, the armature is pulled upward to close the air gap. The mechanical force $\mathbf{F}_e$ of electric origin can once again be found from energy balance.

In the case of the parallel-plate capacitor of Fig. 5.31, we found $\mathbf{F}_e$ in two ways: by keeping the voltage across the plates constant and by keeping the charge on the plates constant. We found that the two approaches resulted in equivalent expressions for the force. In the present case, we can find $\mathbf{F}_e$ by keeping the current I in the exciting coil to be a constant or by keeping the magnetic flux ψ in the core (and, hence, in the air gap) to be a constant. The two approaches should result in equivalent expressions for $\mathbf{F}_e$. We shall, therefore, take advantage of this to simplify the task of finding $\mathbf{F}_e$ by keeping ψ constant, since then no voltage is induced in the coil and, hence, the electrical energy input term in (5.123) can be set to zero. Also, we shall once again assume a lossless system, apply to the armature an external force equal to $-\mathbf{F}_e$, and displace it by an infinitesimal distance in the direction of the external force. Thus, we obtain

$$-F_{ex}\,dx = dW_m$$

$$F_{ex} = -\frac{dW_m}{dx}$$

where W_m is the magnetic stored energy in the system.

Neglecting fringing of flux across the air gap and noting that the displacement of the armature changes only the magnetic energy stored in the air gap, we write the following:

$$H_{\text{gap}} = \frac{\psi}{A\mu_0}$$

$$
\begin{aligned}
(W_m)_{\text{gap}} &= 2\left[\frac{1}{2}\mu_0(H_{\text{gap}})^2 Ax\right] \\
&= \mu_0\left(\frac{\psi}{A\mu_0}\right)^2 Ax \\
&= \frac{\psi^2 x}{A\mu_0}
\end{aligned}
$$

where A is the cross-sectional area of each gap, and the factor 2 takes into account two gaps. Proceeding further, we have

$$
\begin{aligned}
\frac{dW_m}{dx} &= \frac{d}{dx}[(W_m)_{\text{gap}}] \\
&= \frac{\psi^2}{A\mu_0} \\
F_{ex} &= -\frac{\psi^2}{A\mu_0}
\end{aligned}
$$

$$
\boxed{\mathbf{F}_e = -\frac{\psi^2}{A\mu_0}\mathbf{a}_x} \tag{5.129}
$$

The expression for $\mathbf{F}_e$ in terms of the current I in the coil that would result from considerations of constant I may now be found by simply expressing ψ in (5.129) in terms of I. Thus, if we assume for simplicity that the permeability of the magnetic core material is so high that

$$
H_{\text{core}} l_{\text{core}} \ll H_{\text{gap}} l_{\text{gap}}
$$

where l_{core} and l_{gap} are the lengths of the core and air gap, respectively, then

$$
\begin{aligned}
NI &\approx 2H_{\text{gap}}\, x \\
H_{\text{gap}} &\approx \frac{NI}{2x} \\
B_{\text{gap}} &\approx \frac{\mu_0 NI}{2x} \\
\psi &\approx \frac{\mu_0 NIA}{2x}
\end{aligned}
$$

$$
\boxed{\mathbf{F}_e \approx -\frac{\mu_0 N^2 I^2 A}{4x^2}\mathbf{a}_x} \tag{5.130}
$$

Finally, the computation of energy converted from electrical to mechanical, or vice versa, in a magnetic-field electromechanical system can be performed in a manner similar to that illustrated in Example 5.12 for an electric-field system.

K5.7. Mechanical force of electric origin; Energy conversion; Parallel-plate capacitor with movable plate; Electromagnet.

D5.14. For the parallel-plate capacitor of Fig. 5.29, assume $V = 10$ V, $x = 1$ cm, and $A = 0.01$ m^2 and compute $\mathbf{F}_e$ for each of the following cases: (**a**) the dielectric between the plates is free space; (**b**) the dielectric between the plates is a material of permittivity $4\varepsilon_0$; and (**c**) the lower half of the region between the plates is a dielectric of permittivity $4\varepsilon_0$, whereas the upper half is free space.
Ans. **(a)** $-5000\varepsilon_0\mathbf{a}_x$ N; **(b)** $-20{,}000\varepsilon_0\mathbf{a}_x$, N; **(c)** $-12{,}800\varepsilon_0\mathbf{a}_x$ N.

SUMMARY

In this chapter, we first introduced the electric scalar and magnetic vector potential functions, less Φ and $\mathbf{A}$, respectively. From Gauss' law for the magnetic field in differential form, we have

$$\mathbf{B} = \nabla \times \mathbf{A} \tag{5.131}$$

and then from Faraday's law in differential form, we obtain

$$\mathbf{E} = -\nabla\Phi - \frac{\partial \mathbf{A}}{\partial t} \tag{5.132}$$

In (5.132), $\nabla\Phi$ is the gradient of the scalar function Φ. We learned that the gradient of a scalar Φ is a vector having magnitude equal to the maximum rate of increase of Φ at that point, and its direction is the direction in which the maximum rate of increase occurs, that is, normal to the constant Φ surface passing through that point; that is,

$$\nabla\Phi = \frac{\partial \Phi}{\partial n}\mathbf{a}_n$$

In Cartesian coordinates, the expansion for the gradient is

$$\nabla\Phi = \frac{\partial \Phi}{\partial x}\mathbf{a}_x + \frac{\partial \Phi}{\partial y}\mathbf{a}_y + \frac{\partial \Phi}{\partial z}\mathbf{a}_z$$

Next, we derived two differential equations for the potential functions. These are given by

$$\nabla^2\Phi - \mu\varepsilon\frac{\partial^2 \Phi}{\partial t^2} = -\frac{\rho}{\varepsilon} \tag{5.133a}$$

$$\nabla^2\mathbf{A} - \mu\varepsilon\frac{\partial^2 \mathbf{A}}{\partial t^2} = -\mu\mathbf{J} \tag{5.133b}$$

where $\nabla^2\Phi$ is the Laplacian of the scalar Φ and $\nabla^2\mathbf{A}$ is the Laplacian of the vector $\mathbf{A}$. In Cartesian coordinates,

$$\nabla^2\Phi = \frac{\partial^2\Phi}{\partial x^2} + \frac{\partial^2\Phi}{\partial y^2} + \frac{\partial^2\Phi}{\partial z^2}$$

and

$$\nabla^2\mathbf{A} = (\nabla^2 A_x)\mathbf{a}_x + (\nabla^2 A_y)\mathbf{a}_y + (\nabla^2 A_z)\mathbf{a}_z$$

In deriving (5.133a) and (5.133b), we made use of the Lorenz condition

$$\boldsymbol{\nabla}\cdot\mathbf{A} = -\mu\varepsilon\frac{\partial\Phi}{\partial t}$$

which is consistent with the continuity equation.

We then considered the potential functions for the static field case, for which (5.132) reduces to

$$\mathbf{E} = -\boldsymbol{\nabla}\Phi = -\boldsymbol{\nabla}V \tag{5.134}$$

whereas (5.131) remains unaltered. In (5.134), the symbol Φ is replaced by the symbol V, since the electric potential difference between two points in a static electric field has the same meaning as the voltage between the two points. We considered the potential field of a point charge and found that for the point charge

$$V = \frac{Q}{4\pi\varepsilon R} \tag{5.135}$$

where R is the radial distance away from the point charge. The equipotential surfaces for the point charge are thus spherical surfaces centered at the point charge. We illustrated the application of the potential concept in the determination of electric field due to charge distributions by considering the examples of an electric dipole and a line charge. We also discussed a procedure for computer plotting of equipotentials. We then derived the expression for the magnetic vector potential due to a current element. For a current element $I\,d\mathbf{l}$, the magnetic vector potential is given by

$$\mathbf{A} = \frac{\mu I\,d\mathbf{l}}{4\pi R} \tag{5.136}$$

where R is the distance from the current element.

Next, we introduced Poisson's and Laplace's equations. Poisson's equation given by

$$\nabla^2 V = -\frac{\rho}{\varepsilon}$$

is a differential equation governing the behavior of the electric scalar potential in a region of charge, whereas Laplace's equation

$$\nabla^2 V = 0$$

holds in a charge-free region. We discussed the application of Poisson's and Laplace's equations for the solution of problems involving the variation of V with one dimension only. In particular, we illustrated the solution of Poisson's equation by considering the example of a *p-n* junction diode and the solution of Laplace's equation by considering the determination of capacitance for several cases. We then considered the determination of circuit parameters for infinitely long, parallel conductor arrangements. Specifically, (1) we derived the expressions for the capacitance per unit length ($\mathscr{C}$), the conductance per unit length ($\mathscr{G}$), and the inductance per unit length ($\mathscr{L}$) for a coaxial cylindrical arrangement; (2) we showed that the three circuit parameters are related through the material parameters σ, ε, and μ, as given by

$$\frac{\mathscr{G}}{\mathscr{C}} = \frac{\sigma}{\varepsilon}$$

$$\mathscr{L}\mathscr{C} = \mu\varepsilon$$

and (3) we used these relationships for other geometries of the conductors. We then extended our discussions to internal inductance and mutual inductance.

Next, we introduced the quasistatic extension of the static field as a means of obtaining the low-frequency behavior of a physical structure. The quasistatic-field approach involves starting with a time-varying field having the same spatial characteristics as the static field and then obtaining field solutions containing terms up to and including the first power in frequency by using Maxwell's curl equations for time-varying fields. We learned that the quasistatic approximation leads to electric- and magnetic-field systems. We illustrated the quasistatic-field analysis by considering two examples, one of them involving a lossy medium.

We then discussed the magnetic circuit, which is essentially an arrangement of closed paths for magnetic flux to flow around, just as current does in electric circuits. The closed paths are provided by ferromagnetic cores, which, because of their high permeability relative to that of the surrounding medium, confine the flux almost entirely to within the core regions. We illustrated the analysis of magnetic circuits by considering two examples, one of them including an air gap in one of the legs.

Finally, we studied the topic of electromechanical energy conversion. By considering examples of a parallel-plate capacitor with one movable plate, and an electromagnet, we discussed the determination of mechanical forces of electric origin. We also illustrated energy conversion computation for the parallel-plate capacitor example.

REVIEW QUESTIONS

Q5.1. What are electromagnetic potentials? How do they arise?

Q5.2. What is the expansion for the gradient of a scalar in Cartesian coordinates? When can a vector be expressed as the gradient of a scalar?

Q5.3. Discuss the physical interpretation for the gradient of a scalar function and the application of the gradient concept for the determination of unit vector normal to a surface.

Q5.4. How is the Laplacian of a scalar defined? What is its expansion in Cartesian coordinates?

Q5.5. Compare and contrast the operations of curl of a vector, divergence of a vector, gradient of a scalar, and Laplacian of a scalar.

Q5.6. How is the Laplacian of a vector defined? What is its expansion in Cartesian coordinates?

Q5.7. Outline the derivation of the differential equations for the electromagnetic potentials.

Q5.8. What is the relationship between the static electric field intensity and the electric scalar potential?

Q5.9. Distinguish between voltage, as applied to time-varying fields, and the potential difference in a static electric field.

Q5.10. Describe the electric potential field of a point charge.

Q5.11. Discuss the determination of the electric field intensity due to a charge distribution by using the potential concept.

Q5.12. Discuss the procedure for the computer plotting of equipotentials due to two (or more) point charges.

Q5.13. Compare the magnetic vector potential field due to a current element to the electric scalar potential due to a point charge.

Q5.14. State Poisson's equation. How is it derived?

Q5.15. Discuss the application of Poisson's equation for the determination of potential due to the space charge layer in a *p-n* junction semiconductor.

Q5.16. State Laplace's equation. In what regions is it valid?

Q5.17. Discuss the application of Laplace's equation for a conducting medium.

Q5.18. Outline the solution of Laplace's equation in one dimension by considering the variation of potential with x only.

Q5.19. Outline the steps in the derivation of the expression for the capacitance of an arrangement of two conductors.

Q5.20. Discuss the relationship between the capacitance, conductance, and inductance per unit length for an infinitely long, parallel conductor arrangement.

Q5.21. Outline the steps in the derivation of the expressions for the capacitance, conductance, and inductance per unit length of an infinitely long parallel cylindrical-wire arrangement.

Q5.22. Distinguish between internal inductance and external inductance. Discuss the concept of flux linkage pertinent to the determination of the internal inductance.

Q5.23. Explain the concept of mutual inductance and discuss an example of its computation.

Q5.24. What is meant by the quasistatic extension of the static field in a physical structure?

Q5.25. Outline the steps involved in the quasistatic extension of the static field in a parallel-plate structure short-circuited at one end.

Q5.26. Discuss the derivation of the condition for the validity of the quasistatic approximation for the parallel-plate structure short-circuited at one end.

Q5.27. Discuss the general condition for the quasistatic approximation of a physical structure.

Q5.28. Discuss the classification of physical structures as electric- and magnetic-field systems.

Q5.29. Discuss the low-frequency behavior of a parallel-plate structure with a lossy medium between the plates.

Q5.30. Discuss the quasistatic behavior of the structure of Fig. 5.20 for $\sigma \approx 0$.

Q5.31. What is a magnetic circuit? Why is the magnetic flux in a magnetic circuit confined almost entirely to the core?

Q5.32. Define the reluctance of a magnetic circuit. What is the analogous electric circuit quantity? Why is the reluctance for a given set of dimensions of a magnetic circuit not a constant?

Q5.33. Discuss the complete analogy between a magnetic circuit and an electric circuit using the example of the toroidal magnetic core versus the toroidal conductor.

Q5.34. How is the fringing of the magnetic flux in an air gap in a magnetic circuit taken into account?

Q5.35. Discuss by means of an example the analysis of a magnetic circuit with three legs and its equivalent-circuit representation.

Q5.36. Discuss by means of an example the phenomenon of electromechanical energy conversion.

Q5.37. Outline the computation of mechanical force of electric origin from considerations of energy balance associated with an electromechanical system.

Q5.38. Discuss by means of an example the computation of energy converted from electrical to mechanical, or vice versa, in an electromechanical system.

PROBLEMS

Section 5.1

P5.1. **Two identities in vector calculus.** Show by expansion in the Cartesian coordinate system that: **(a)** $\boldsymbol{\nabla} \cdot \boldsymbol{\nabla} \times \mathbf{A} = 0$ for any $\mathbf{A}$ and **(b)** $\boldsymbol{\nabla} \times \boldsymbol{\nabla}\Phi = \mathbf{0}$ for any Φ.

P5.2. **Application of identities in vector calculus.** Determine which of the following vectors can be expressed as the curl of another vector and which of them can be expressed as the gradient of a scalar:

(a) $xy\mathbf{a}_x + yz\mathbf{a}_y + zx\mathbf{a}_z$

(b) $(1/r^2)(\cos\phi\,\mathbf{a}_r + \sin\phi\,\mathbf{a}_\phi)$ in cylindrical coordinates

(c) $(1/r)\sin\theta\,\mathbf{a}_\phi$ in spherical coordinates.

P5.3. **Finding a scalar function for which the gradient is a given vector function.** Find the scalar functions whose gradients are given by the following vector functions:

(a) $e^{-y}(\cos x\,\mathbf{a}_x - \sin x\,\mathbf{a}_y)$

(b) $(\cos\phi\,\mathbf{a}_r - \sin\phi\,\mathbf{a}_\phi)$ in cylindrical coordinates

(c) $(1/r^3)(2\cos\theta\,\mathbf{a}_r + \sin\theta\,\mathbf{a}_\theta)$ in spherical coordinates

P5.4. Application of the gradient concept. By using the gradient concept, show that the unit vector along the line of intersection of two planes

$$a_1x + a_2y + a_3z = c_1$$
$$b_1x + b_2y + b_3z = c_2$$

which are not parallel is given by

$$\pm \frac{(a_2b_3 - a_3b_2)\mathbf{a}_x + (a_3b_1 - a_1b_3)\mathbf{a}_y + (a_1b_2 - a_2b_1)\mathbf{a}_z}{\sqrt{(a_2b_3 - a_3b_2)^2 + (a_3b_1 - a_1b_3)^2 + (a_1b_2 - a_2b_1)^2}}$$

Then find the unit vector along the intersection of the planes $x + y + z = 3$ and $y = x$.

P5.5. Application of the gradient concept. By using the gradient concept, show that the equation of the plane passing through the point (x_0, y_0, z_0) and normal to the vector $(a\mathbf{a}_x + b\mathbf{a}_y + c\mathbf{a}_z)$ is given by

$$a(x - x_0) + b(y - y_0) + c(z - z_0) = 0$$

Then find the equation of the plane tangential to the surface $xyz = 1$ at the point $(\frac{1}{2}, \frac{1}{4}, 8)$.

P5.6. Laplacian of a vector in cylindrical coordinates. Show that the Laplacian of a vector in cylindrical coordinates is given by

$$\nabla^2\mathbf{A} = \left(\nabla^2 A_r - \frac{A_r}{r^2} - \frac{2}{r^2}\frac{\partial A_\phi}{\partial \phi}\right)\mathbf{a}_r + \left(\nabla^2 A_\phi - \frac{A_\phi}{r^2} + \frac{2}{r^2}\frac{\partial A_r}{\partial \phi}\right)\mathbf{a}_\phi + (\nabla^2 A_z)\mathbf{a}_z$$

Section 5.2

P5.7. Equipotential surfaces and direction lines of electric field for a given electric potential. For the static electric potential function $V(x, y) = xy$, discuss the equipotential surfaces and the direction lines of the electric field with the aid of sketches.

P5.8. Electric potential and field for a rectangular quadrupole. An arrangement of point charges known as the rectangular quadrupole consists of the point charges Q, $-Q$, Q, and $-Q$, at the points $(0, 0, 0)$, $(\Delta x, 0, 0)$, $(\Delta x, 0, \Delta z)$, and $(0, 0, \Delta z)$, respectively. Obtain the approximate expression for the electric potential and hence for the electric field intensity due to the rectangular quadrupole at distances r from the origin large compared to Δx and Δz.

P5.9. Electric potential for a finitely long line charge. For a finitely long line charge of uniform density ρ_{L0} C/m situated along the line between $(0, 0, -a)$ and $(0, 0, a)$, obtain the expression for the electric potential at an arbitrary point (r, ϕ, z) in cylindrical coordinates. Further show that the equipotential surfaces are ellipsoids with the ends of the line as their focii.

P5.10. Electric potential for two parallel infinitely long line charges. Show that for two infinitely long line charges parallel to the z-axis, having uniform densities $\rho_{L1} = 2k\pi\varepsilon_0$ C/m and $\rho_{L2} = -2\pi\varepsilon_0$ C/m and passing through $(-1, 0, 0)$ and $(1, 0, 0)$, respectively, the potential is given by $V = \ln(r_2/r_1^k)$, where r_1 and r_2 are distances to the point from the line charges 1 and 2, respectively.

P5.11. Electric potential at the center of a rectangular uniformly distributed surface charge. Consider the surface charge distributed uniformly with density ρ_{S0} C/m^2

on a rectangular-shaped surface of sides a and b. Show that the electric potential at the center of the rectangle is

$$\frac{\rho_{S0}}{2\pi\varepsilon_0}\left(a \ln \frac{\sqrt{a^2 + b^2} + b}{a} + b \ln \frac{\sqrt{a^2 + b^2} + a}{b}\right)$$

Further show that for a square-shaped surface of sides a, the potential at the center is $(\rho_{S0}a/\pi\varepsilon_0) \ln (1 + \sqrt{2})$.

P5.12. Potential difference in the field of an infinitely long strip of surface charge. Consider surface charge of uniform density ρ_{S0} C/m^2 distributed on an infinitely long strip lying between the straight lines $x = -a, y = 0$ and $x = a, y = 0$. Noting that the electric potential is independent of z, show that the potential difference between two points in the first quadrant of the xy-plane $(x_1, y_1, 0)$ and $(x_2, y_2, 0)$ is given by

$$\begin{aligned}\frac{\rho_{S0}}{4\pi\varepsilon_0}\Big\{&(a - x_2) \ln [(a - x_2)^2 + y_2^2] + (a + x_2) \ln [(a + x_2)^2 + y_2^2] \\ &- (a - x_1) \ln [(a - x_1)^2 + y_1^2] - (a + x_1) \ln [(a + x_1)^2 + y_1^2] \\ &+ 2y_2\left(\tan^{-1} \frac{a - x_2}{y_2} + \tan^{-1} \frac{a + x_2}{y_2}\right) \\ &- 2y_1\left(\tan^{-1} \frac{a - x_1}{y_1} + \tan^{-1} \frac{a + x_1}{y_1}\right)\Big\}\end{aligned}$$

P5.13. Magnetic vector potential and field for a magnetic dipole. Consider a circular current loop of radius a lying in the xy-plane with its center at the origin and with current I flowing in the sense of increasing ϕ, so that the magnetic dipole moment $\mathbf{m}$ is $I\pi a^2\,\mathbf{a}_z$. Show that far from the dipole such that $r \gg a$, the magnetic vector potential is given by

$$\mathbf{A} \approx \frac{\mu\mathbf{m} \times \mathbf{a}_r}{4\pi r^2}$$

and hence the magnetic flux density is given by

$$\mathbf{B} = \frac{\mu m}{4\pi r^3}(2 \cos\theta\,\mathbf{a}_r + \sin\theta\,\mathbf{a}_\theta)$$

P5.14. An identity in vector calculus. By expansion in Cartesian coordinates, show that

$$\mathbf{A} \times \nabla\Phi = \Phi\nabla \times \mathbf{A} - \nabla \times (\Phi\mathbf{A})$$

Section 5.3

P5.15. Solution of Poisson's equation for a space-charge distribution in Cartesian coordinates. A space-charge density distribution is given by

$$\rho = \begin{cases} -\rho_0\left(1 + \dfrac{x}{d}\right) & \text{for } -d < x < 0 \\ \rho_0\left(1 - \dfrac{x}{d}\right) & \text{for } 0 < x < d \\ 0 & \text{otherwise} \end{cases}$$

where ρ_0 is a constant. Obtain the solution for the potential V versus x for all x. Assume $V = 0$ for $x = 0$.

P5.16. Solution of Poisson's equation for a space-charge distribution in Cartesian coordinates. A space-charge density distribution is given by

$$\rho = \begin{cases} \rho_0 \sin x & \text{for } -\pi < x < \pi \\ 0 & \text{otherwise} \end{cases}$$

where ρ_0 is a constant. Find and sketch the potential V versus x for all x. Assume $V = 0$ for $x = 0$.

P5.17. Solution of Poisson's equation for a space-charge distribution in spherical coordinates. A space-charge density distribution is given in spherical coordinates by

$$\rho = \begin{cases} \rho_0 & \text{for } \quad a < r < 2a \\ 0 & \text{otherwise} \end{cases}$$

where ρ_0 is a constant. Find and sketch the potential V versus r for all r.

P5.18. Solution of Laplace's equation for a parallel-plate capacitor with two perfect dielectrics. The region between the two plates in Fig. 5.10 is filled with two perfect dielectric media having permittivities ε_1 for $0 < x < t$ (region 1) and ε_2 for $t < x < d$ (region 2). **(a)** Find the solutions for the potentials in the two regions $0 < x < t$ and $t < x < d$. **(b)** Find the capacitance per unit area of the plates.

P5.19. Solution of Laplace's equation for a parallel-plate capacitor with imperfect dielectrics. Assume that the two media in Problem P5.18 are imperfect dielectrics having conductivities σ_1 and σ_2 for $0 < x < t$ and $t < x < d$, respectively. **(a)** What are the boundary conditions to be satisfied at $x = t$? **(b)** Find the solutions for the potentials in the two regions. **(c)** Find the potential at $x = t$.

P5.20. Parallel-plate capacitor with a dielectric of nonuniform permittivity. Assume that the region between the two plates of Fig. 5.10 is filled with a perfect dielectric of nonuniform permittivity

$$\varepsilon = \frac{\varepsilon_0}{1 - (x/2d)}$$

Find the solution for the potential between the plates and obtain the expression for the capacitance per unit area of the plates.

P5.21. Coaxial cylindrical capacitor with a dielectric of nonuniform permittivity. Assume that the region between the coaxial cylindrical conductors of Fig. 5.11(a) is filled with a dielectric of nonuniform permittivity $\varepsilon = \varepsilon_0 b/r$. Obtain the solution for the potential between the conductors and the expression for the capacitance per unit length of the cylinders.

Section 5.4

P5.22. Capacitance per unit length of parallel wire line with large spacing between the wires. For the parallel-wire arrangement of Fig. 5.13(c), show that for $d \gg a$, the capacitance per unit length of the line is $\pi\varepsilon/\ln(2d/a)$. Find the value of d/a for which the exact value of the capacitance per unit length is 1.05 times the value given by the approximate expression for $d \gg a$.

P5.23. Direction lines of electric field for a parallel-wire line. For the line-charge pair of Fig. 5.15, show that the direction lines of the electric field are arcs of circles emanating from the positively charged line and terminating on the negatively charged line.

P5.24. Inductance of a toroid with magnetic core. A filamentary wire carrying current I is closely wound around a toroidal magnetic core of rectangular cross section, as shown in Fig. 5.32. The mean radius of the toroidal core is a and the number of turns per unit length along the mean circumference of the toroid is N. Find the inductance of the toroid.

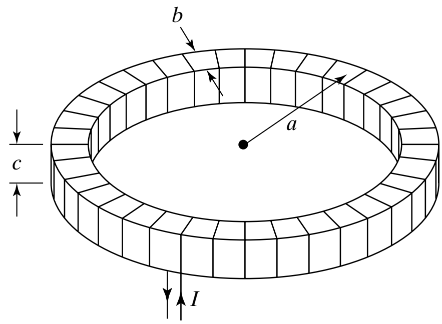

FIGURE 5.32

For Problem P5.24.

P5.25. Inductance per unit length of an infinitely long, uniformly wound solenoid. An infinitely long, uniformly wound solenoid of radius a and having N turns per unit length carries a current I. Find the inductance per unit length of the solenoid. Assume air core ($\mu = \mu_0$).

P5.26. Internal inductance per unit length of a wire with nonuniform current distribution. A current I flows with nonuniform volume density given by

$$\mathbf{J} = J_0\left(\frac{r}{a}\right)^2 \mathbf{a}_z$$

along an infinitely long cylindrical conductor of radius a having the z-axis as its axis. The current returns with uniform surface density in the opposite direction along the surface of an infinitely long, perfectly conducting cylinder of radius b $(> a)$ and coaxial with the inner conductor. Find the internal inductance per unit length of the inner conductor.

P5.27. Magnetic energy stored in an infinitely long cylindrical conductor of current. Consider the infinitely long solid cylindrical conductor of Fig. 5.16. Obtain the expression for the energy stored per unit length in the magnetic field internal to the current distribution and show that it is equal to $\frac{1}{2}\mathcal{L}_i I^2$, where I is the total current.

P5.28. Mutual inductance per unit length of two coaxial solenoids. An infinitely long, uniformly wound solenoid of radius a and having N_1 turns per unit length is coaxial with another infinitely long, uniformly wound solenoid of radius b $(> a)$ and having N_2 turns per unit length. Find the mutual inductance per unit length of the solenoids. Assume air core ($\mu = \mu_0$).

Section 5.5

P5.29. Input behavior of an inductor at low and high frequencies. For the structure of Fig. 5.19, assume that $l = 10$ cm, $d = 5$ mm, and $w = 5$ cm and free space for the medium between the plates. **(a)** For a current source $I(t) = 1 \cos 10^6 \pi t$ A, find the voltage developed across the source. **(b)** Repeat part (a) for $I(t) = 1 \cos 10^9 \pi t$ A.

P5.30. Frequency behavior of a capacitor beyond the quasistatic approximation. For the structure of Fig. 5.20 with $\sigma = 0$, show that the input behavior for frequencies slightly beyond those for which the quasistatic approximation is valid is equivalent to the series combination of $C(= \varepsilon wl/d)$ and $\frac{1}{3}L$, where $L = \mu\, dl/w$ is the inductance of the structure obtained from static-field considerations with the two plates joined by another conductor at $z = 0$, as in Fig. 5.19.

P5.31. Quasistatic input behavior of a resistor for three different cases. Find the conditions under which the quasistatic input behavior of the structure of Fig. 5.20 is essentially equivalent to that of: **(a)** a single resistor; **(b)** a capacitor $C(= \varepsilon wl/d)$ in parallel with a resistor; and **(c)** a resistor in series with an inductor.

P5.32. Frequency behavior of an inductor with material having nonzero conductivity. For the structure of Fig. 5.19, assume that the medium has nonzero conductivity σ. **(a)** Show that the input behavior correct to the first power in ω is the same as if σ were zero. **(b)** Investigate the input behavior correct to the second power in ω and obtain the equivalent circuit.

P5.33. Frequency behavior of an inductor beyond the quasistatic approximation. For the structure of Fig. 5.19, obtain the equivalent circuit for the input behavior for frequencies for which the fields up to and including the fifth-order terms in ω are significant.

Section 5.6

P5.34. Calculations involving a toroidal magnetic core. A toroidal magnetic core has the dimensions $A = 5\ \text{cm}^2$ and $l = 20$ cm. **(a)** If it is found that for NI equal to 200 A-t, a magnetic flux ψ equal to 8×10^{-4} Wb is established in the core, find the permeability μ of the core material. **(b)** If now an air gap of width $l_g = 0.1$ mm is introduced, find the new value of NI required to maintain the flux of 8×10^{-4} Wb, neglecting fringing of flux in the air gap.

P5.35. Calculations involving a magnetic circuit with three legs and an air gap. For the magnetic circuit of Fig. 5.27, assume the air gap to be in the center leg. Find the NI required to establish a magnetic flux of 9×10^{-4} Wb in the air gap.

P5.36. Calculations involving a magnetic circuit with three legs and two air gaps. For the magnetic circuit of Fig. 5.27, assume that there is an air gap of length 0.2 mm in the left leg in addition to that in the right leg. Find the NI required to establish a magnetic flux of 4×10^{-4} Wb in the air gap in the right leg.

P5.37. Magnetic circuit with a center leg and two symmetrical side legs. For the magnetic circuit of Fig. 5.27, assume that there is no air gap. Find the magnetic flux established in the center leg for an applied NI equal to 180 A-t.

P5.38. Magnetic circuit with a center leg and two asymmetrical side legs. For the magnetic circuit of Fig. 5.27, assume that there is no air gap and that $A_1 = 5\ \text{cm}^2$, with all other dimensions remaining as specified in Example 5.1. Find the magnetic flux density in the center leg for an applied NI equal to 150 A-t.

Section 5.7

P5.39. Finding the mechanical force of electric origin for a parallel-plate capacitor system. In Fig. 5.33, a dielectric slab of permittivity ε sliding between the plates of a parallel-plate capacitor experiences a mechanical force $\mathbf{F}_e$ of electrical origin. Assuming width w for the plates normal to the page and neglecting fringing of fields at the edges of the plates, find the expression for $\mathbf{F}_e$.

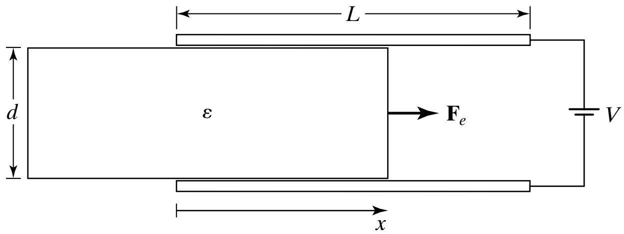

FIGURE 5.33

For Problem P5.39.

P5.40. Finding the mechanical force of electric origin for a cylindrical capacitor system. In Fig. 5.34, a dielectric material of permittivity ε sliding freely in a cylindrical capacitor experiences a mechanical force $\mathbf{F}_e$ of electrical origin in the axial direction. Show that

$$\mathbf{F}_e = \frac{V_0^2\pi(\varepsilon - \varepsilon_0)}{\ln(b/a)}\mathbf{a}_x$$

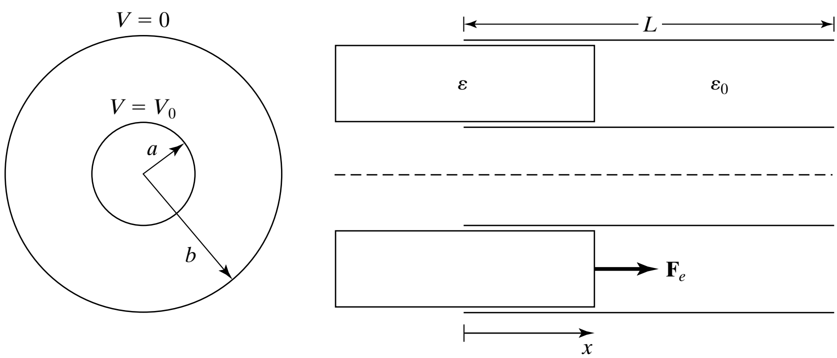

FIGURE 5.34

For Problem P5.40.

P5.41. Energy conversion in a parallel-plate capacitor with a movable plate. Assume that in Example 5.12, the parallel-plate capacitor system of Fig. 5.29 is made to traverse the closed cycle in the V-x plane shown in Fig. 5.35 instead of the closed cycle in the Q-x plane shown in Fig. 5.30. Calculate the energy converted per cycle and determine whether the conversion is from mechanical to electrical or vice versa.

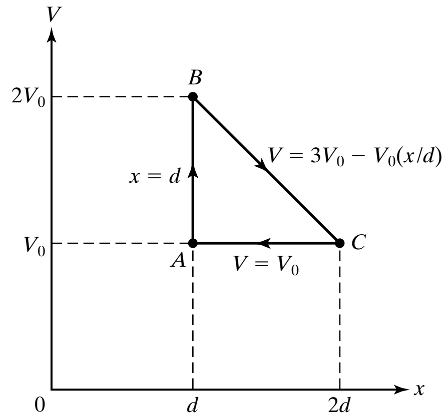

FIGURE 5.35
For Problem P5.41.

P5.42. Energy conversion in a solenoidal coil with sliding magnetic core. Figure 5.36(a) shows a magnetic-field electromechanical device in which the magnetic core is free to slide inside a long air-core solenoidal coil. The solenoid has length l, radius a, and number of turns per meter N, and carries a current I. The magnetic core has length $b < l$, radius a, and permeability $\mu \gg \mu_0$, and extends a distance x into the solenoid. **(a)** Neglect fringing of the field and find the mechanical force $\mathbf{F}_e$ of electric origin on the core. Plot F_{ex} versus x. **(b)** Assume that the device is

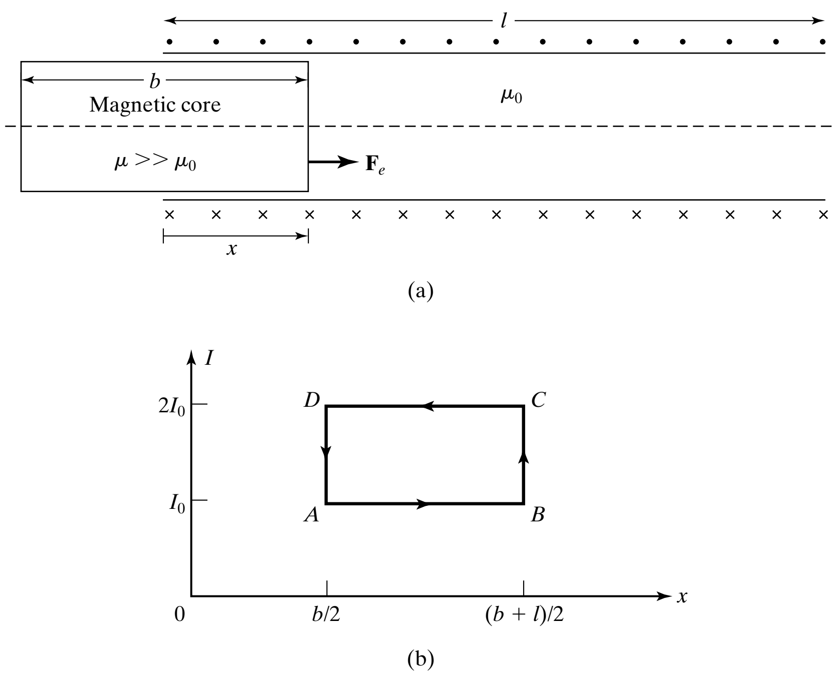

FIGURE 5.36
For Problem P5.42.

made to traverse the closed path in the I-x plane, as shown in Fig. 5.36(b). Find the energy converted per cycle and determine whether it is from mechanical to electrical or vice versa.

REVIEW PROBLEMS

R5.1. Finding the angle between two planes by using the gradient concept. By using the gradient concept, show that the angle α between two planes

$$a_1x + a_2y + a_3z = c_1$$
$$b_1x + b_2y + b_3z = c_2$$

is given by

$$\alpha = \cos^{-1}\frac{a_1b_1 + a_2b_2 + a_3b_3}{\sqrt{(a_1^2 + a_2^2 + a_3^2)(b_1^2 + b_2^2 + b_3^2)}}$$

Then find the angle between the planes $x + y + z = 1$ and $z = 0$.

R5.2. Electric potential due to a circular charged disk of uniform charge density. Consider a circular disk of radius a lying in the xy-plane with its center at the origin and carrying charge of uniform density ρ_{S0} C/m^2. Obtain the expression for the potential V due to the charged disk at a point $(0, 0, z)$ on the z-axis. Verify your answer by considering the limiting cases of $V(z)$ for $|z| \gg a$ and $E_z(z)$ for $|z| \ll a$.

R5.3. Magnetic vector potential and field for an infinitely long straight wire of current. Obtain the magnetic vector potential at an arbitrary point due to an infinitely long straight filamentary wire lying along the z-axis and carrying a current I in the $+z$-direction. Then evaluate $\mathbf{B}$ by performing the curl operation on the magnetic vector potential.

R5.4. Spherical capacitor with a dielectric of nonuniform permittivity. Assume that the region between the concentric spherical conductors of Fig. 5.11(b) is filled with a dielectric of nonuniform permittivity $\varepsilon = \varepsilon_0 b^2/r^2$. Obtain the solution for the potential between the conductors and the expression for the capacitance.

R5.5. Finding the internal inductance per unit length of a cylindrical conductor arrangement. Current I flows with uniform density along an infinitely long, hollow cylindrical conductor of inner radius a and outer radius b and returns with uniform surface density in the opposite direction along the surface of an infinitely long, perfectly conducting cylinder of radius c $(> b)$ and coaxial with the hollow conductor. Find the internal inductance per unit length of the arrangement.

R5.6. Quasistatic input behavior of a short-circuited coaxial cable. An air-dielectric coaxial cable of inner radius $a = 1$ cm, outer radius $b = 2$ cm, and length $l = 1$ m is short-circuited at one end. Obtain the equivalent circuit for the input behavior of the structure for frequencies slightly beyond those for which the quasistatic approximation is valid. Compute the resonant frequency of the equivalent circuit and comment on its value compared to those for which the circuit is valid.

R5.7. Calculations involving a magnetic circuit with three legs. For the magnetic circuit shown in Fig. 5.37, the dimensions of the legs are $A_1 = A_3 = 2$ cm^2, $A_2 = 3$ cm^2, $l_1 = l_3 = 30$ cm, and $l_2 = 10$ cm. The permeability of the core material

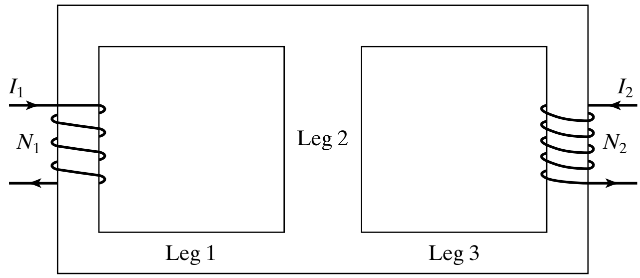

FIGURE 5.37

For Problem R5.7.

can be assumed to be $1000\mu_0$. **(a)** Draw the equivalent electric circuit. **(b)** For $N_1I_1 = 200$ A-t and $N_2I_2 = 100$ A-t, find the magnetic flux in each leg.

R5.8. For analyzing an electromechanical system set in motion. In the system shown in Fig. 5.38, the mass M is set in motion in the following manner: (1) the mass is brought to rest at the equilibrium position $x = x_0$ with no charge on the capacitor plates; (2) the mass is constrained to that position and the capacitor plates are charged to $\pm Q$ as shown; and (3) the mass is released, thereby permitting frictionless motion. Obtain the differential equation for the motion of M and find the solution.

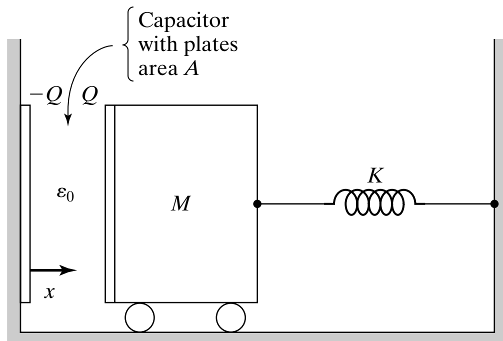

FIGURE 5.38

For Problem R5.8.